

**Best
Available
Copy**

AD-A008 853

LONG RANGE MATERIALS RESEARCH

Robert A. Huggins

Stanford University

Prepared for:

Defense Advanced Research Projects Agency

31 December 1974

DISTRIBUTED BY:

NTIS

National Technical Information Service
U. S. DEPARTMENT OF COMMERCE

SEMI-ANNUAL TECHNICAL REPORT

July 1, 1974 - December 31, 1974

Long Range Materials Research

Sponsored by
Defense Advanced Research Projects Agency
ARPA Order No. 2470 - Amendment F

Program Code Number: 4D10

Contractor: Stanford University

Effective Date of Contract: June 1, 1974

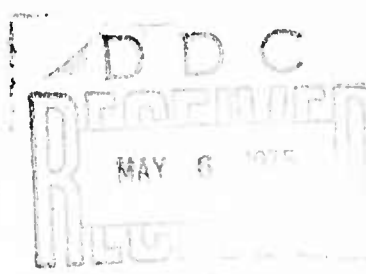
Contract Expiration Date: May 31, 1975

Amount of Grant: \$164,000

Grant Number: DAI C15 73 C15 Amendment No. 2

Principal Investigator: Robert A. Huggins
Phone: (415) 497-4118

Short Title: Long Range Materials Research



The views and conclusions contained in this document are those of the authors and should not be interpreted as necessarily representing the official policies, either expressed or implied, of the Defense Advanced Research Projects Agency or the U. S. Government.

Reproduced by
**NATIONAL TECHNICAL
INFORMATION SERVICE**
U.S. Department of Commerce
Springfield, VA. 22151

Center for Materials Research
Stanford University
Stanford, California 94305
(415) 497-4118

TABLE OF CONTENTS

	Page
I. INTRODUCTION	1
II. DETECTION OF X-RADIATION	3
C. W. Bates, Jr.	
1. Introduction	4
2. Optical Properties of CsI and CsI(Na)	4
3. References	7
III. SUPERPLASTICITY AND WARM WORKING OF PLAIN HIGH CARBON STEELS	8
O. D. Sherby, J. C. Shyne	
A. <u>Development of Superplastic Ultra-High-Carbon Steels by Special Thermal Mechanical Processing</u>	9
O. D. Sherby, B. Walser, C. M. Young, L. M. Cady	
1. Introduction	9
2. Superplasticity in Ultra High Carbon Steels	11
3. Development of Ultra Fine Equiaxed Structures	14
4. Room Temperature Mechanical Properties of Ultra High Carbon Steels Containing Fine Structures	24
5. Heat Treatment of Fine-Structure Ultra High Carbon Steels	25
6. Ultra High Carbon Steels, A Summary	26
7. References	27
B. <u>Breakdown of Lamellar Microstructures</u>	28
J. C. Shyne	
IV. SYNTHESIS OF NEW TYPES OF CATALYST MATERIALS	31
J. P. Collman, M. Boudart, W. A. Little	
A. <u>Heterogenized Homogeneous Catalysts</u>	32
1. Heterogenized-Homogenized Hydrogenation Catalysts	32
2. Metallic Catalyst Supports	33
3. Face to Face Porphyrin Synthesis	33
4. References	34

B.	<u>Supported Multimetallic Clusters</u>	35
1.	Structure of Small Metallic Particles	35
2.	Supported Iron Samples: Chemisorption	36
3.	Structure Sensitivity of Ammonia Synthesis on Iron	36
4.	Surface Magnetic Anisotropy of Small Ion Particles	37
5.	Conclusion	37
6.	References	38
C.	<u>Preparation of Fine Particles</u>	39
	W. A. Little, J. W. Brill	
V.	DEVELOPMENT OF ELEVATED TEMPERATURES ELECTROCRYSTALLIZATION TECHNIQUES	41
	R. S. Feigelson, R. A. Huggins	
A.	<u>Introduction</u>	42
B.	<u>Investigation of the LaB₆ System</u>	44
	I. V. Zubeck, P. A. ⁶ Pettit	
1.	Introduction	44
2.	Experimental Results	44
3.	Future Work	47
4.	References	48
C.	<u>Continuous Growth</u>	49
	R. DeMattei	
1.	Introduction	49
2.	Experimental Results	50
3.	Future Plans	53
4.	References	54

I. INTRODUCTION

I. INTRODUCTION

This semi-annual technical report on the research program entitled "Long Range Materials Research," covers the period June 1, 1974 through December 31, 1974. This program is composed of four separate programs as follows:

1. Detection of X-Ray Radiation
2. Superplasticity and Warm Working of Metals and Alloys
3. Synthesis of New Types of Catalyst Materials
4. Development of Elevated Temperature Electro-crystallization Techniques

Progress in each of the subareas during this report period will be described separately in the succeeding sections of this report.

II. DETECTION OF X-RADIATION

C. W. Bates, Jr.

Associate Professor of Materials Science
and Engineering
and Electrical Engineering

II. DETECTION OF X-RADIATION

1. Introduction

The work in our laboratory is aimed at determining the physics of the luminescence phenomena associated with activated and unactivated alkali halide crystals which are used as particle detectors in high energy physics¹⁻⁹, x-ray sensors in astronomical observations¹⁰ and in the medical field in x-ray image intensifiers used in diagnostic radiology¹¹. Our work is currently concentrated on unraveling the luminescent mechanism in CsI(Na), at present the most efficient alkali x-ray converter (x-ray photons to blue light photons). During this report period we feel that we have made a significant breakthrough in determining certain aspects of this mechanism.

2. Optical Properties of CsI and CsI(Na)

Initially it was felt that there was a fundamental luminescence at room temperature associated with pure CsI. However as higher purity materials became available, it became obvious that this luminescence could be associated with trace impurities such as thallium or sodium or that the crystal had been deformed or strained in some fashion. The work of Towyama¹² has shown that there is a luminescence peaking at 300 and 415 nm upon excitation by beta rays in specimens of CsI which have been heated in air at 500°C for one half an hour and then quenched on an aluminum plate to room temperature.

A question that arises in connection with this work is the amount of

impurities in the specimens used. Towyama states that the crystals were prepared by the vacuum Bridgman method without subsequent refining. Further, his emission spectra at room and liquid nitrogen temperatures look suspiciously like the spectra we have obtained for films of CsI(Na) prepared under various conditions, such as mole percent of sodium and heat treatment after the film has been evaporated onto suprasil-quartz substrates. We have examined "research pure" crystals of CsI from the Harshaw Chemical Company which they prepare by a proprietary process. They examine 3" to 4" thick specimens of this material in emission spectroscopy to check for impurities and find none. Dr. Carl Swinehart of Harshaw informs me that these are the purest crystals of CsI that he has ever examined. We examined three of these crystals (1/2" x 1/2" x 2mm) and found no emission at room temperature from two of them and a very weak emission from the third one which was just above the noise level with our excitation and emission apparatus adjusted for maximum sensitivity. A difference in the handling of these three crystals could have produced this result. However one can begin to say with some assurance that there is no (very little) room temperature luminescence from CsI.

CsI(Na) on the other hand has a room temperature emission with λ_{max} at 425 nm with a narrow excitation band centered at 252 nm. That this is the only emission was checked by looking for different excitation spectra for wavelengths under the emission curve with λ_{max} at 4250 Å. None was found. At liquid nitrogen temperature an emission at 340 nm appears which is most efficiently excited in the excitonic region around 215 nm, the emission at 425 nm being considerably reduced over that at room temperature. Upon heating the "research pure" CsI to 500°C in dry nitrogen and cooling to room temperature in about 8 hours we were able to reproduce the excitation and emission spectra for CsI(Na) at room and

liquid nitrogen temperatures very closely i.e., λ_{max} is 430 nm instead of 425 nm and the excitation spectrum has its maximum at 245 instead of 252 nm. At liquid nitrogen temperatures the 340 nm emission is excited most efficiently at 220 instead of 215 nm. Unlike Towyama we did not have any emission at 300 nm at room temperature. The spectra are the same as regards shape and intensity for measurements made on equally thick samples (2mm). The "research pure" CsI spectra was slightly broader.

Our heat treatment of the "research pure" CsI cannot be considered an annealing process^{*}. We must then assume that our treatment resulted in the production of a large number of vacancies. The suggestion then follows that sodium in CsI introduces vacancies. To the best of our knowledge this is the first experiment to demonstrate this effect in this manner. Other treatments^{13,14} have drawn the analogy with CsI doped with divalent cations which exhibit similar but not identical luminescence. These divalent cations must introduce alkali cation vacancies for charge neutrality. The addition of divalent cations to CsI is difficult and involves the risk of contamination. Our results have involved only the use of ultra pure CsI without the addition of any impurities and we have reproduced the CsI(Na) spectra as regards shape intensity and temperature dependence of the emission at 425 nm. The differences obtained with the divalent cations from that with sodium are to be expected as in order to get any effect we must have on the order of 200 ppm of divalent impurities, whereas with the sodium 6 ppm is optimum.

* To properly anneal CsI one raises the temperature 1 degree per hour from room temperature to 500°C and then lowers the temperature to room temperature at the same rate. We are grateful to Dr. Swinehart for conveying this information to us.

3. References

1. R. Hofstadter, Phys. Rev. 74, 100 (1948); 75, 976 (1949).
2. H. Kallmann, Phys. Rev. 75, 623 (1949).
3. E. C. Farmer, H. B. Moore and C. Goodman, Phys. Rev. 76, 454 (1949).
4. C. E. Mandeville and H. O. Albrecht, Phys. Rev. 80, 299 (1950).
5. R. Hofstadter, J. A. McIntyre and H. I. West, Phys. Rev. 82, 749 (1951).
6. M. Furst and H. Kallman, Phys. Rev. 82, 964 (1951).
7. J. Bonanomi and J. Rossel, Helv. Phys. Acta. 25, 725 (1952).
8. W. Van Sciver and R. Hofstadter, Phys. Rev. 87, 522 (1952).
9. B. Hahn and J. Rossel, Helv. Phys. Acta. 26, 271, 803 (1953).
10. F. S. Mozer, E. Bogott and C. W. Bates, Jr., IEEE Trans. on Nucl. Sci. NS-15, 144 (1968).
11. C. W. Bates, Jr., Adv. in Electronics and Electron Physics, 28A, 545 (1969).
12. T. Towyama, Physics Letters 31A, 206 (1970).
13. A. Panova et al, Prikl. Spektrosk 6, 549 (1967).
14. A. Panova and N. Shiran, Izv. Akad. Nauk SSSR, Ser. Fiz. 31, 859 (1967).

III. SUPERPLASTICITY AND WARM WORKING
OF PLAIN HIGH CARBON STEELS

O. D. Sherby

Professor of Materials Science
and Engineering

and

J. C. Shyne

Professor of Materials Science
and Engineering

A. Development Of Superplastic Ultra-High-Carbon Steels by Special Thermal Mechanical Processing

Oleg D. Sherby, Bruno Walser, Conrad M. Young and Eldon M. Cady

1. Introduction

For many applications, the ideal structural metallic material needs the following qualities for its fabrication, application and extensive use. During fabrication it should be capable of deforming to large strains without cracking and under small externally applied forces for minimum expenditure of energy. For final use as a structural material it should be strong, tough and possess high ductility. The third important requirement is that it should be inexpensive. Such a combination of properties is not generally achievable in most metallic systems and it is the objective of the materials scientist and engineer to reach such utopian goals. We have obtained the above sought for properties in ordinary steels containing carbon as the only principal alloying element; other elements like manganese, silicon, and sulfur are present at the same concentration as in scrap steel. We found the desired properties by adding a higher carbon content (1.3 to 2.3%C) than is normally used industrially for making plain carbon steels and we have developed unusual and special processing operations to obtain the desired final microstructure.

Steels containing 1.1 to 2.3% carbon have rarely, if ever, been considered for broad industrial applications. Such steels would be classified between what is known as high carbon steel ($\approx 1.1\%C$) and cast iron ($\approx 1.7\%C$). Normally they are considered as potentially too brittle for ambient temperature application and their high temperature characteristics apparently have not been explored. It is steels in this very composition range that we have made superplastic at warm temperatures (0.4 to $0.6T_m$ where T_m is the absolute melting temperature)

and strong and ductile at room temperature.

The concept of adding large amounts of carbon, in the form of cementite, to steel and the development of special thermal-mechanical processing procedures towards the attainment of unique properties and microstructure were conceived and developed by us at Stanford. We wish to point out, however, that the special structures we have created may possibly have been produced, perhaps accidentally, over 1000 years ago. The damascus steels of ancient Persia and India, also called bulat steels, are known to have high carbon contents, commonly 1.5 to 2.0% carbon. The high quality of these steels is well established. Their manufacture, however, appears to be a forgotten art and there is considerable uncertainty with regard to the origin of the "damask" or "watering" structure observed visually on the surface of damascus blades and swords. Many of the early metallurgists speculated in depth on the possible relation of the visual structure obtained to the corresponding mechanical properties. Much speculation centered on the possible importance of melting procedure, rate of cooling, purity content and mechanical treatment on the resulting properties and structure; apparently the only common point of agreement on the prerequisites for a good blade or sword was that the carbon content should be high. Smith and Beliaev^(1,2) cover the controversy on these steels in detail. We would like to relate the following remarkable historical documentation on damascus (bulat) steels. P. Anasov, a major-general in the Russian Army and superintendent of the Zlatoust Steel Works in the Ural mountains, devoted his whole life to trying to understand how bulat steels were made by the Persians and Indians. He wrote a treatise on this subject, apparently a life-time study, entitled "On the Bulat", in 1841⁽³⁾. His enthusiasm for such high carbon steels prompted him to forecast that "—our agricultural laborers will till the soil with damascene ploughshares, our artisans will use tools fashioned of damascene steel, and damascene steel will

supersede all steel now employed for the manufacture of articles of special hardness and endurance". Apparently his enthusiasm for such steels was not shared by contemporary steel industry for no new ultra high carbon steels seemed to have appeared on the technological scene, at least not in large quantity. It is, thus, with some trepidity that we share Anasov's enthusiasm of a century and a quarter ago⁽⁴⁾. Perhaps our new findings, based on our ability to control the microstructure and based on our understanding of deformation mechanisms and processes at elevated and low temperatures, will lead to a permanent use for ultra high carbon steels for many technological applications. The following is a description of our results which is to be the basis of a patent that we have submitted to the patent office at Stanford University.

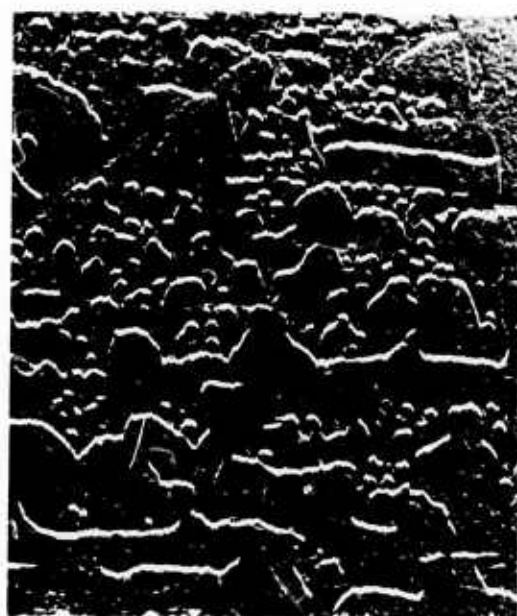
2. Superplasticity in Ultra High Carbon Steels

Our motivation for considering ultra high carbon contents in steels was primarily to increase its ease of formability at warm temperatures. Research on model alloy systems⁽⁵⁾ has revealed that certain prerequisites are generally needed for superplastic behavior and high formability at warm temperatures. These are: fine stable grains with equiaxed structure and two phases with each phase having about the same strength at the working temperature (generally about 10 to 50 volume percent of second phase). It is our contention that these attributes exist in hypereutectoid steels if one is able to produce the second phase (cementite) in fine spheroidized form. Such fine spheroidized structures have been developed for a eutectoid composition steel (0.8%C) and some researchers^(7,8) have attributed superplastic behavior to it. We do not concur with this conclusion since only about 100% elongation was observed in slow rate tension tests. We have also worked extensively with such carbon steels and have not been able to make it

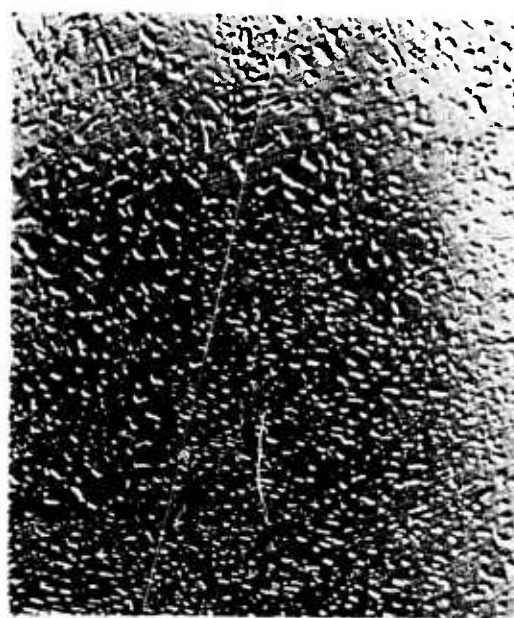
superplastic^(9,10). We define a material as superplastic if the strain rate sensitivity exponent, m , in the relation $\sigma = K\dot{\epsilon}^m$, (σ is the flow stress, $\dot{\epsilon}$ is the strain rate and K is a material constant) is equal to or greater than 0.4 and elongations in the order of 500% are achieved. We believe that one reason why a eutectoid composition steel cannot readily be made superplastic is due to the ease of grain growth at warm temperatures (i.e. at temperatures around 650°C). It is well established that the tendency for superplastic flow diminishes with an increase in grain size. Thus grain growth inhibits superplasticity. A eutectoid composition steel contains about 12 volume percent cementite. Generally, superplasticity is enhanced when the volume fraction of second phase is increased. This is partly because grain growth is made more difficult and partly because more phase boundaries are introduced and these can contribute to plastic flow by grain boundary shearing, a mode of deformation which apparently dominates the superplastic flow process. Our new idea was to work with steels containing 1.3% to 1.9% (20 to 29 volume percent cementite) and we have been able to prepare material containing one micron size grains which remain fine during plastic flow at warm temperatures. Such materials exhibit high values of the strain rate sensitivity exponent, m , in the order of 0.4, and elongations approaching 500% when tested high in the ferrite range (650°C, $T = .5T_m$). Such elongations were achieved in tests performed at strain rates as high as 10% per minute.

Several methods of developing fine structures will be described later. The fine spheroidized structures attainable in ultra high carbon steels by our specially developed processing methods are illustrated in Figure 1. As can be seen the massive cementite phase present in the original castings is broken up by extensive working of the steels at warm temperatures. An example illustrating the superplastic behavior of the ultra high carbon steels, when in fine spheroidized form,

1.6 % CARBON STEEL



AS - CAST



AFTER WARM WORKING

5 μ m

1.9 % CARBON STEEL



AS - CAST



AFTER WARM WORKING

5 μ m

Figure 1. The above carbon replica electron photomicrographs illustrate the influence of warm working on the breakup of the original massive cementite particles in cast ultra-high carbon steels (left photomicrographs). Extensive warm working yielded a fully spheroidized structure in the 1.6% carbon steel (upper right). Considerable refinement of the structure also occurred in the 1.9% carbon steel (lower right) but because it was not as extensively worked some cementite plates are still present.

is shown in Figure 2. As can be seen these steels exhibit very high ductility at 650°C. An example of a 1.9%C steel twisted rapidly (in 5 seconds) at 650°C is shown in Figure 3, revealing uniform plastic flow with no fracturing. Such behavior would suggest that superplastic-like deformation mechanisms are taking place in these ultra high carbon steels. We have examined the microstructure of our material after extensive plastic flow and have found that the grain size remains fine and equiaxed. An example for the 1.9%C steel, using transmission electron microscopy, is shown in Figure 4, where it can be seen that the grain size of the ferrite matrix is equiaxed and equal to about 2 microns. The bulbous nature of the cementite particles is reflective of the high degree of mobility of this phase at 650°C allowing it to accommodate to the large change in sample geometry from plastic straining. Such behavior is typical of superplastic two phase alloys⁽⁵⁾. It is our belief that the presence of manganese and other impurities (e.g., silicon) at the levels common to commercial steels assist the spheroidized cementite in maintaining the fine grain size of the iron and thus its superplastic properties.

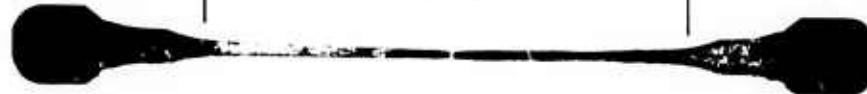
We were not able to achieve m values as high as 0.5 in the ferrite-cementite range of temperatures, a value generally associated with perfect superplastic behavior. This suggested that we had not quite optimized either our microstructure or our conditions of testing. We knew that another important variable in superplasticity of two phase metallic systems is the relative strength of each of the two phases. If the second phase (cementite in our case) is hard the material will not be superplastic. The strengths of the two phases should be nearly the same at the temperature where superplastic flow is to occur⁽⁷⁾. The hardness of cementite is not known as a function of temperature but we know it is readily deformable at 650°C. We speculated that cementite may be somewhat harder than

UNDEFORMED SAMPLE

GAGE
LENGTH



470 %



1.3 % C STEEL

470 %



1.6 % C STEEL


340 %



1.9 % C STEEL

0 2 4 6 8 10 12 cm.

Figure 2. Superplastic flow of ultra high carbon steels at 650°C, deformed at an engineering strain rate of 1% per minute.



1.9% carbon steel: warm
rolled to a plate at
 650°C (1200°F), then
twisted at 650°C (1200°F).

Figure 3. The above photograph illustrates the ease of twisting a sample of superplastic 1.9% carbon steel at 650°C .



Figure 4. Transmission electron micrograph of spheroidized 1.9%C steel after 100% elongation at 650°C, deformed at 1% per minute. The fine equiaxed grain size of about 2 μ m and the bulbous shape of the cementite is typical of superplastically deformed microstructures.

the ferrite matrix at 650°C and decided to study the mechanical behavior of our ultra high carbon steels at 800°C. At this temperature, iron has transformed to austenite with a strength about equal to ferrite at 650°C.⁽¹¹⁾ The cementite phase, however, should be considerably weaker due to the normal effect of temperature on strength. The grain size of the transformed austenite should be very fine and there should be sufficient cementite remaining to stabilize the grains during superplastic flow. The volume fraction of cementite at 800°C need not be as high as at 650°C because grain growth is inhibited in austenite by the low rate of iron self-diffusion in the close packed face-centered cubic structure⁽¹²⁾. As we expected, our ultra high carbon steels exhibit superplasticity in the gamma-cementite range at 800°C ($T = 0.6T_m$) with m equalling 0.5. Even at high deformation rates the steels exhibit high m values; at an engineering strain rate of 100% per minute we were able to obtain tensile elongations up to 170%.

Our findings thus indicate that ultra high carbon steels (0.9 to 2.3%C) can be exceptionally formable at warm temperatures. These steels can be worked extensively (and our rolling experiments reveal this clearly) in the ferrite plus cementite range (600 to 720°C, and even as low as 500°C). Shaping at such temperatures has the added advantage that very little oxidation occurs during working with very little buildup of an oxide scale. Shaping of our ultra high carbon steels now in the gamma plus cementite range (720 to 900°C) is slightly more advantageous especially for the manufacture of complex shapes since it is nearly perfectly superplastic here. The temperature is higher, however, which leads to slightly higher surface oxidation as well as to an added expense in heating.

3. Development of Ultra Fine Equiaxed Structures

An essential feature of superplastic materials is that they exhibit an ultra fine equiaxed structure with grain sizes in the order of one micron. This, then,

was the task facing us in our attempt to develop fine equiaxed structures in our ultra high carbon steels. Once developed they are then ready for superplastic forming either in the ferrite or austenite range of temperatures.

We have developed several methods of obtaining fine spheroidized structures of cementite in a matrix of fine ferrite grains. Among them are the following:

First Method

In a "first method" for forming the ultra high carbon steels of the present invention, a steel plate, billet, or any other form of steel, is first homogenized in the gamma range by heating to a temperature at which substantially all of the carbon present in the cementite is dissolved in the austenite (gamma iron) matrix. A suitable temperature for this purpose is on the order of 1100 to 1150°C. By reference to the Iron-carbon phase diagram, it is apparent that with a carbon content in substantial excess of 2%, the carbon content is too high to be completely dissolved in the austenite. As defined herein, homogenization will include heating a steel with a carbon content in excess of 2% to a temperature high in the gamma-cementite range (e.g., 50°C below the melting point of 1147°C). The purpose of homogenization is to place the carbon and other elements present into a relatively uniform solution. This assists in the formation of a uniform fine grained iron structure after working.

In a second step according to the first method, the steel plate is then mechanically worked in the gamma range to break up the cast structure. This is an optional step. As defined herein, mechanical working includes rolling, forging, extrusion, or any other procedure which subjects the steel to sufficient deformation to form the aforementioned microstructure. The purpose of mechanical working in the gamma range is to accelerate homogenization and refine the austenite grains which might otherwise tend to agglomerate and form larger grain structure. This may

reduce the requirement for subsequent mechanical working to accomplish the desired fine grained structure with spheroidized cementite.

In the next step, the steel plate is mechanically worked to a substantial extent during cooling through the gamma-cementite range. It is preferable that such working be continuous. This working comminutes the pro-eutectoid cementite into a finer spheroidized form as it is precipitated from solution. Mechanical working also contributes to refining further the austenite grain. The level of mechanical working varies depending upon a number of factors including the prior processing history of the steel. A typical amount of deformation in the gamma-cementite range is a true strain level (ϵ) on the order of 1.5. A practical measure of such strain is the deformation produced during a size reduction of a 5:1 ratio.

In a final step of the first method, the steel is again mechanically worked, as by rolling, at a temperature high in the ferrite-cementite range. Strains of the foregoing order of magnitude are employed in this temperature not only further to spheroidize the cementite structure but also to reduce the size of the pearlite structure formed during the gamma-alpha transformation. Temperatures employed for such mechanical working are on the order of 500 to 720°C. At the lower end of the range the steel can possibly alligator. Accordingly, it is preferable that this mechanical working take place above this temperature as in a range from 600 to 720°C.

A steel formed in accordance with the foregoing process includes an iron grain matrix with uniformly dispersed cementite. The iron grain is stabilized in a predominantly equiaxed fine grained configuration. The cementite is in predominantly spheroidized form at cold to elevated temperatures. For economy of operation and uniformity of the microstructure, it is preferable to mechanically work the steel continuously from temperatures in the gamma-cementite range through

temperatures high in the alpha-cementite range.

In a "first alternative method", the mechanical working in the alpha-cementite range is eliminated so that the primary mechanical working is in the gamma-cementite range. The result of this procedure is as follows. During mechanical working in the gamma-cementite range, essentially all of the cementite is converted to the spheroidized form. However, during transformation of the iron from the gamma to the alpha form on cooling, the austenite containing dissolved carbon is converted to ferrite plus additional cementite in non-spheroidized form, typically plates. As set forth above, it is important that essentially all of the cementite be in spheroidized form at the temperature of fabrication in order for the steel to be highly plastic at that temperature. Accordingly, at temperatures below the gamma-alpha transformation (723°C) the presence of substantial non-spheroidized cementite greatly reduces the plasticity of the steel processed in accordance with this alternative procedure. However, by heating the steel to a temperature above the alpha-gamma transition (723°C) most of non-spheroidized cementite and all of the alpha iron is reconverted to austenite iron containing dissolved carbon with a large portion of the remaining cementite in spheroidized form. This material is again rendered superplastic.

The first alternative method is to be contrasted to the first method in which the steel is mechanically worked in the alpha-cementite range. In the first method, essentially all of the cementite which is present in the steel in the alpha-cementite range is converted to spheroidized form. That steel is superplastic at typical temperature of fabrication on either side of the gamma-alpha conversion (e.g., $600-900^{\circ}\text{C}$).

We give an example of the type of microstructure and mechanical properties obtained by the thermal mechanical processing describing as the first method. A

casting of the 1.3%C steel was heated to 1130°C for 60 minutes and then was rolled continuously, in twelve passes, at 10% per pass, to a true strain to 1.2. Since the original casting cooled during rolling it experienced deformation in the gamma range as well as gamma plus cementite range. When a temperature of 650°C was reached it was rolled isothermally in this ferrite plus cementite range to an additional true strain of 1.2 (again, at 10% per pass). The microstructure of the warm worked steel, given in Figure 5, revealed a fine spheroidized structure with ferrite grains in the order of one micron and less. The room temperature properties of the material were as follows: (1) the Rockwell "C" hardness of the plate was 34, and (2) tensile tests revealed a yield strength of 147 ksi, an ultimate tensile strength of 182 ksi and tensile elongation of 7% (one inch gage length sample). The high temperature properties reveal this material to be superplastic with 482% elongation to fracture at 650°C when deformed at a strain rate of one percent per minute.

Second Method

In a "second method", the steel is treated in a manner similar to the first method including homogenization in the gamma range and mechanical working in the gamma-cementite range. The details of these procedures are incorporated at this point by reference. Thereafter, at a temperature low in the gamma-cementite range, (e.g., 750-850°C), the steel plate is rolled isothermally to form a fine grained iron. Since this steel is highly plastic at such temperature, it can be worked extensively without cracking. Thereafter, the steel may be processed according to conventional techniques. For example, the rolled casting can be air cooled to room temperature for storage. The microstructure of this rolled steel includes fine pearlite with spheroidized cementite. Isothermal working at 800°C has the advantage that refining of the iron grain and spheroidizing of the cementite occurs at a



Figure 5. Carbon replica photomicrograph illustrating fine spheroidized microstructure in a 1.3%C steel as obtained by extensive warm working following the procedure described in the first method.

controlled and fixed temperature and can yield a strong tough material. Since this material has a fine structure at room temperature, it can be reheated at a subsequent time to temperatures at which it can be fabricated into the desired configuration in a superplastic state. A preferred temperature for such final working is low in the gamma-cementite range. This heating across the gamma-alpha transition removes most of the non-spheroidized cementite which had precipitated in plate form during cooling. The different microstructure formed by working in the alpha-cementite and gamma-cementite range are set forth in the section on the first method.

The steel, isothermally worked in the gamma plus cementite range, is made superplastic below 723°C by deforming it to large strains (e.g. $\epsilon = 1.5$) in the alpha plus cementite range (e.g. 600 to 700°C). As stated in the first method this deformation process will spheroidize the transformation product obtained from cooling the steel isothermally worked previously in the gamma-cementite range.

An example of the microstructure and properties obtained by the second method is as follows. A 1.6% carbon casting was homogenized at 1100°C for 60 minutes. It was then forged in the gamma plus cementite range (cooling to about 800°C), in ten steps, to a total true strain of 2.0. The forged plate was then rolled isothermally at 850°C to a total true strain of 2.0 (at twenty percent per pass with 5 minute reheating time between passes) and then air cooled. The microstructure of this steel, shown in Figure 6, reveal the presence of proeutectoid cementite in spheroidized form and transformation product consisting of fine pearlite. The room temperature properties of this material gave a Rockwell "C" hardness of 30. In compression tests at room temperature, the plate exhibited a yield strength of 190 ksi, with no cracking occurring up to 30% compression strain.

If the above processed steel is heated to 650°C and isothermally worked at this

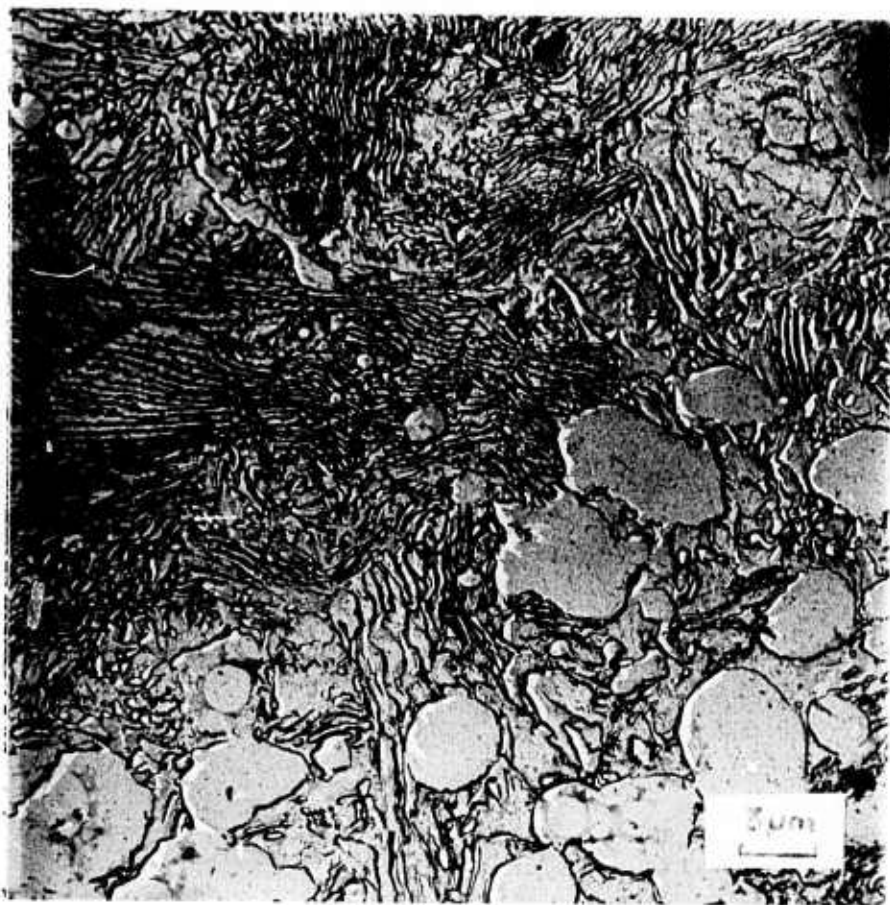


Figure 6. Carbon replica photomicrograph illustrating proeutectoid cementite and pearlite in a 1.6%C steel after extensive working in the gamma-cementite range. The steel was processed as described in the second method.

temperature to a true strain of $\epsilon = 1.2$, the result is a microstructure as shown in Figure 7. Much of the transformation product is now spheroidized and the result is a strong material with a room temperature hardness of Rockwell "C" 37.

Third Method

In a "third method", the ultra high carbon steel is heated into the gamma range for homogenization in accordance with the principles of the foregoing first and second methods. Here, the steel is rapidly cooled through the alpha-gamma transformation to form martensite plus retained austenite. Thereafter, the steel is tempered to a suitable temperature high in the alpha-cementite range, e.g., 650°C. As a last step, this tempered martensite-containing steel is warm worked in the alpha-cementite range to break up and spheroidize the cementite precipitated from the retained austenite. As a precaution against cracking, the quenching rate should be controlled. One technique is to employ an oil quench rather than a water quench for this purpose.

The third method may have a number of important advantages. Firstly, the formation of martensite creates a relatively fine microstructure which thus reduces the amount of working required to refine the grain size. In addition, the final product is extremely strong at room temperature and is characterized by superplasticity at temperatures of 600-900°C which can be employed for fabrication. The structure of this steel at room temperature includes fine grained iron and cementite in predominantly spheroidized form.

In an alternative to the third method, mechanical working may be accomplished in the gamma-cementite range rather than warm working in the alpha-cementite range. For optimum plasticity, fabrication of a steel produced according to this alternative is accomplished in the gamma-cementite range.

An example of the microstructure obtained by the third method is given in Figure 8. This fine spheroidized structure was obtained in a 1.6%C steel using the



Figure 7. Carbon replica photomicrograph illustrating a 1.6%C steel processed in the same way as described in Figure 6 except for additional working in the alpha-cementite range.

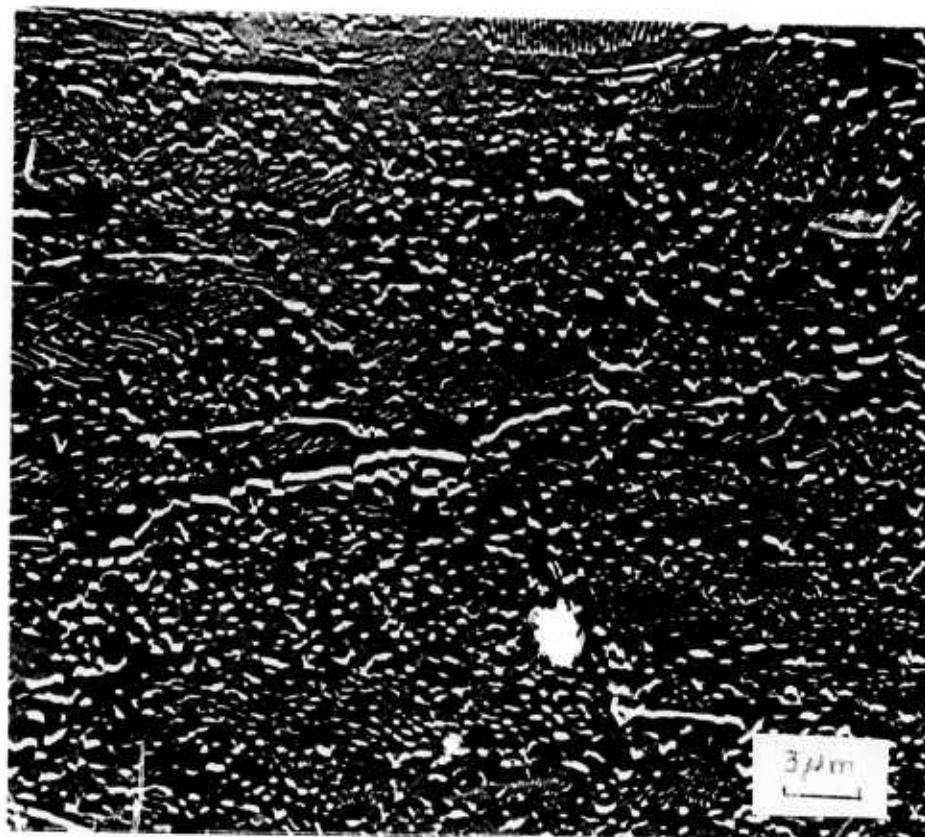


Figure 8. Carbon replica photomicrograph illustrating the fine spheroidized microstructure obtained by extensive working at 550°C of a quenched and tempered 1.6%C steel as described in the third method.

following procedure. The casting was homogenized at 1130°C for 60 minutes and water quenched. It was then heated to 550°C for 2 hours and rolled isothermally at this temperature to a strain of 1.8. The fineness of the structure obtained at the low warm working temperature resulted in a high room temperature hardness of Rockwell "C" 50.

Fourth Method

In a "fourth method" total mechanical working takes place at cold temperatures. It employs part of the procedure of the third method. Thus, the ultra high carbon steel plates are homogenized in the gamma range and then quenched. These plates are then tempered under conditions to obtain an annealed product. Suitable conditions for annealing are temperatures high in the alpha-cementite range, e.g., 700°C, for a time on the order of one-half hour to 2 hours. This annealed product is then cooled to room temperature. Then, the product is mechanically worked, as by rolling, to impose a part of the deformation required to spheroidize essentially all of the cementite and refine the grain size to the desired extent in the subsequent annealing treatment. It is preferable not to impose the total amount of deformation required for this purpose in a single cold rolling because of the possibility of cracking at room temperature. After the first step, the steel is reheated and annealed suitably at the foregoing conditions in order to cause recovery and refinement of the structure. Then this cycle is repeated until the desired total strain is applied.

Thermal cycling through the gamma-alpha transformation temperature at say, 600-800°C, will accelerate the recovery process. In an alternative to the fourth method, the steel may be annealed low in the gamma-cementite range followed by slow cooling (e.g., air cooling) to room temperature. This material can be cold rolled to impart part of the total deformation. Thereafter, this cycle of annealing

and cold working is repeated several times until the desired total deformation is accomplished.

It is apparent that both the fourth method and the alternative fourth method require longer times and more careful control than the first, second and third methods. Thus, in general, the first three methods are preferable ones.

An example of the type of product obtained by the fourth method is given for a 1.3%C steel. The original casting was heated to 1100°C for 90 minutes and subsequently quenched in water. It was then annealed at 700°C for 45 minutes, air cooled and cold rolled to a strain of 0.3. It was again annealed at 700°C for 30 minutes, air cooled and further rolled at room temperature to an additional strain of 0.5. A final annealing treatment at 700°C for 30 minutes was given in order to recover the cold worked structure. Figure 9 illustrates the fine structure obtained by this cyclic annealing, cold-working and annealing treatment of a high carbon steel quenched from the gamma range. This material is relatively soft (Rockwell "C" 20) because of the high annealing temperature in the alpha plus cementite range.

Fifth Method

In a "fifth method", a steel billet is first homogenized in the gamma range and mechanically worked in the same range to break up the cast structure. As set forth in the section on the first method, mechanical working in the gamma range is optional. It accomplishes acceleration of material homogenization and so may be referred to as "mechanical homogenization".

After mechanical working in the gamma range, the worked structure is cooled directly to a warm temperature in the alpha-cementite range and mechanically worked at this temperature to form a fine structure of spheroidized cementite in a fine grained iron matrix. In essence, this procedure accomplishes the total deformation required for this purpose in the alpha-cementite range rather than in a combination

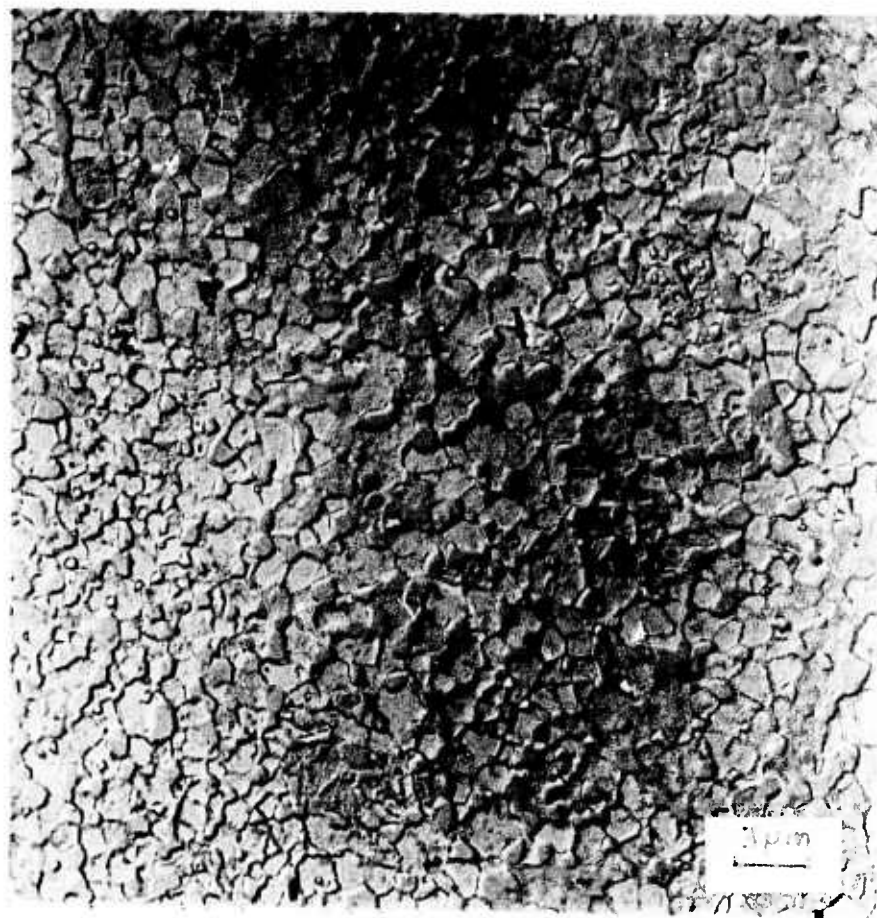


Figure 9. Carbon replica photomicrograph illustrating the fine spheroidized structure in a 1.3%C steel obtained by repetitive cold working and annealing treatments as described in the fourth method.

of gamma-cementite and alpha-cementite range as set forth in the first and second methods. Suitable warm working temperatures in the alpha range are from a minimum of 500°C to the transformation temperature (723°C) and preferably at least 600°C.

In an alternative to the fifth method, mechanical working may be accomplished in the gamma-cementite range rather than warm working in the alpha-cementite range. For optimum plasticity, fabrication of a steel produced according to this alternative is accomplished in the gamma-cementite range.

The fine structure obtained by the fifth method is given as follows for a 1.6%C steel. The original casting was homogenized at 1130°C for 60 minutes and worked at this temperature to a true strain of 1.0. It was then cooled and worked isothermally at 600°C to a true strain of 1.5. The resulting microstructure is shown in Figure 10 where it can be readily seen that a very fine spheroidized structure was obtained. Its room temperature hardness was Rockwell "C" 48. After annealing the rolled product at 650°C for 30 minutes, its room temperature hardness decreased to Rockwell "C" 37. The yield strength of the annealed product was 166 ksi with a total elongation of 3%.

Other techniques may be employed to form the ultra high carbon steel of the foregoing invention so long as the desired microstructure is obtained. One possible technique is to accomplish the desired deformation by thermal cycling between temperatures across the alpha-gamma transformation. It would be necessary to repeat this cycling many times because each stage of such temperature deformation is relatively small compared to that accomplished by mechanical working.

Another technique which may be employed to form a steel of the desired microstructure is powder metallurgical mixing of powders of iron alloys containing spheroidized cementite and fine iron powders. For example, fine powders (e.g., 1-10 micron size) of white cast iron (4 to 5% carbon) can be mixed with iron powders

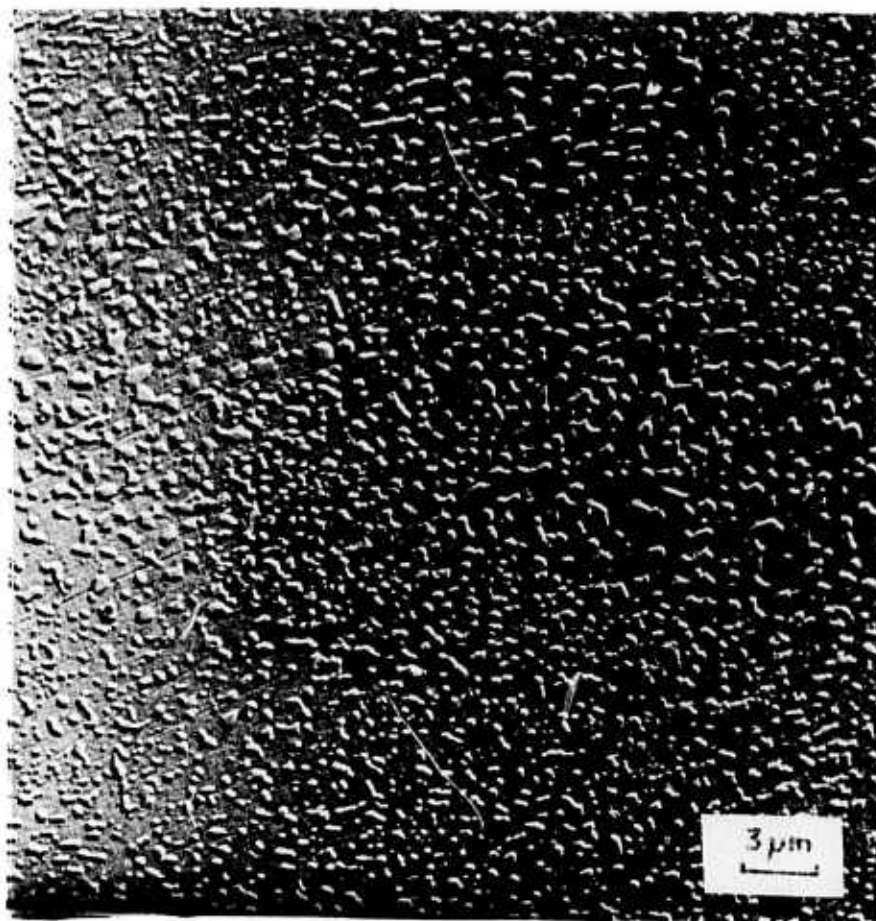


Figure 10. Carbon replica photomicrograph illustrating the fine spheroidized structure in a 1.6%C steel after isothermal working at 600°C as described in the fifth method.

of approximately the same size and pressed and sintered at 600-700°C to bond the powders by solid state fusion. The proportions are selected to conform to the foregoing total carbon contents (e.g., 2 parts of iron to 1 part of white cast iron). Commercial steel impurities including manganese may be supplied in the iron powders or white cast iron powder. The final product has a microstructure with superplastic characteristics at elevated temperatures.

4. Room Temperature Mechanical Properties of Ultra High Carbon Steels Containing Fine Structures

Our success in obtaining fine structures in the ultra high carbon steels is most gratifying. We attribute the superhigh ductility observed at warm temperatures to the presence of these fine structures. Furthermore, we have already indicated that such steels can be strong and ductile at room temperature. The most promising results have been obtained with the 1.3%C steel. In Figure 11 we illustrate the true stress-true strain curve for the 1.3%C steel after warm working at 565°C. The as-warm worked material has a yield strength of about 195,000 psi, a 215,000 psi ultimate tensile strength and 4% tensile elongation which is a very attractive combination of properties. The ductility can be improved by annealing with a resultant decrease in the yield strength. Thus, annealing for 100 hours at 500°C resulted in a yield strength of 150,000 psi and in a ductility of 15% (uniform) elongation. This would indicate that we may have developed a very tough material.

Steels containing carbon contents higher than 1.3%C exhibit yield strengths higher than those we have reported for the 1.3%C steel. This is because the yield strength is principally a function of the mean free path for dislocation motion. Garland⁽¹³⁾ has shown that the yield strength follows a linear relation with $\lambda^{-1/2}$ where λ is the mean distance between obstacles. For high carbon steels the appropriate distance for λ is the mean distance between particles. It can be readily shown that, for a given particle size (about 0.25 μ m) the mean particle spacing

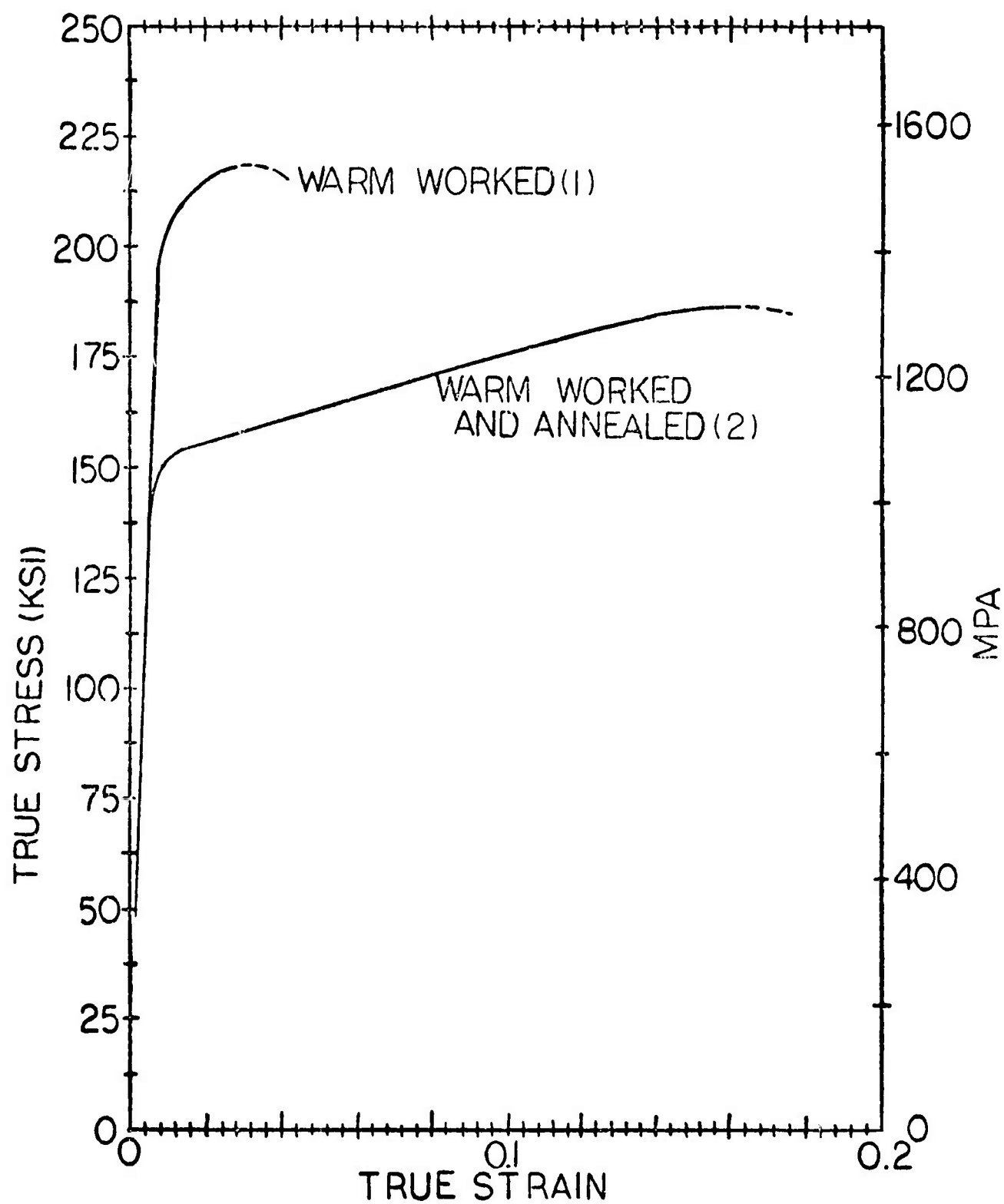


Figure 11. True stress-true strain curves for the Fe-1.3%C alloy at room temperature after warm working at 565°C (1050°F) and (2) after annealing following warm working (500°C for 100 hrs.).

changes from 0.4 μ m for the 1.3%C steel to 0.34 μ m for the 1.6%C steel and 0.29 μ m for the 1.9%C steel. This means that yield strengths of about 160,000 psi can be achieved for an annealed 1.6% steel and about 175,000 psi for an annealed 1.9%C steel. The ductility will remain high with increasing carbon content since the ferrite grain size is fine and this factor dominates the plasticity of the material. Even more impressive yield strengths are obtainable upon further reduction of the particle size. Thus, a particle size of 0.1 micron will result in a yield strength of about 235,000 psi for the 1.3%C steel, 255,000 psi for the 1.6%C steel and 280,000 psi for the 1.9%C steel.

5. Heat Treatment of Fine-Structure Ultra High Carbon Steels

We already indicated that annealing the 1.3%C steel after extensive warm working leads to a considerable increase in ductility (Figure 11). Other heat treatments can be even more useful. After superplastic working or warm working in the alpha range the ultra high carbon steels can be thermally treated to obtain high strength by heating above the critical temperature (723°C) followed by controlled rates of cooling (or quenching to specific isothermal temperatures). In this manner fine grained austenite can be transformed to various forms of transformed structures such as coarse and fine pearlite, coarse and fine bainite, martensite, and so forth.

We wish to point out that heat treatment after superplastic working of fine structures would be especially useful with ultra high carbon steels containing alloying elements. For example, much greater control of the rate of transformation is possible with a 1.5% Cr steel than with plain carbon steels. This, in turn, will permit greater flexibility in obtaining a desired final microstructure. Such steels, however, because of the added cost of alloying, may find less use for applications in contrast to the inexpensive ultra high plain carbon steels which should find wide general utility.

6. Ultra High Carbon Steels, A Summary

Our research has centered on plain carbon steels containing 1.3 to 2.3% carbon (twenty to thirty-five volume percent cementite respectively). Much of our basic studies in the past years related to strain-enhanced spheroidization, warm working, strain created vacancies and superplasticity proved indispensable in our attempt to obtain fine grained structures in ultra high carbon steels. Various TMT (thermal mechanical processing) procedures have been developed which have resulted in particulate composites of cementite in iron containing ferrite grains finer than one micron in size. Such high carbon steels are superplastic at warm temperatures (about 500% elongation have been achieved). Furthermore, they can be made strong and ductile at room temperature; for example, a 1.3% carbon steel, processed to consist of fine spheroidized cementite with accompanying fine ferrite grains, exhibits a yield strength of 150 ksi, and ultimate tensile strength of 205 ksi and 15 percent elongation. To the best of our knowledge this is the first time plain carbon steels have been made superplastic and our results suggest exciting possibilities in the application of inexpensive steels for many new structural application.

7. References

1. C. S. Smith, A History of Metallography, University of Chicago Press, 1960.
2. N. Belaiew, J. Iron and Steel Inst., 97, 1918, 417.
3. P. Anassoff, On the Bulat, Gorny Journal, Russia, 1841; reprinted in its appendix, the "Annuaire du Journal des Mines en Russie", 1843; also published by Ermann in his Archiv für Wissenschaftliche Kunde Von Russland, vol ix, p. 510.
4. We are grateful to Mr. Alan Miller for his bringing to our attention (in the summer of 1974) the early work of Persians, Indians and others on the preparation of high carbon steels, especially as described in references (1) and (2) above.
5. O. D. Sherby, Science Journal, 5, 1969, 75.
6. O. D. Sherby, M. J. Harrigan, L. Chamagne and C. Sauve, Transactions, ASM, 62, 1969, 575.
7. A. R. Marder, Trans. AIME, 245, 1969.
8. G. R. Yoder and Volker Weiss, Metallurgical Transactions, 3, 1972, 675.
9. Conrad Young, Donald Bly and Oleg D. Sherby, Semi-annual progress report to American Iron and Steel Institute, Feb. 1, 1972 - July 31, 1972, Department of Materials Science and Engineering, Stanford University, Stanford, Calif., 94305.
10. First Semi-Annual Technical Report, July 1 - December 31, 1973, Long Range Materials Research, DAHC15 73 G15, Center for Materials Research, Stanford University, Stanford, California 94305.
11. W. Chubb, Trans. AIME, 203, 1955, 189.
12. O. D. Sherby and P. M. Burke, Progress in Materials Science, 13, 1968, 325.
13. J. Gurland, Second International Conference on the Strength of Metals and Alloys, Asilomar, California Conference, ASM, 30 August - 4 September 1970.

B. BREAKDOWN OF LAMELLAR MICROSTRUCTURES

J. C. Shyne

The intent of this portion of the program is to gain information about the kinetics and mechanisms of the spheroidization of lamellar microstructures as a consequence of plastic deformation and thermal activation. The material chosen for study was the 60Sn-40Pb eutectic. This material is interesting for its own sake, since the Sn-Pb eutectic is an important microstructural feature of common solder. However, the main motivation for choosing 60Sn-40Pb as an experimental material is because the Sn-Pb eutectic resembles the more technologically important Fe-C eutectoid, pearlite. The spheroidization of pearlite is an extremely important process in steel technology, but the eutectoid pearlite is experimentally difficult because of the brittleness of the Fe_3C phase of the pearlite at temperatures below about 600°C.

Experimental alloys of the 60Sn-40Pb eutectic have been prepared by melting and casting. By controlling the solidification rate by slow cooling, beautifully well formed lamellar eutectic structures were obtained. Metallographic practices were developed for observing these microstructures.

The intent was to cold work the eutectic alloys at temperatures too low for any thermally activated breakdown of the lamellar structure to a spheroidized equiaxed microstructure, and then to follow the subsequent thermally activated process of spheroidization at some higher temperatures, hopefully above room temperature. Samples were cold rolled at temperatures down to -196°C (liq. N_2), and subsequently their microstructures were examined at room temperature. In all cases, no matter how rapidly the metallography was performed, there was extensive spheroidization of the cold worked specimens. This effectively rules out normal metallography (at room temperature) as a viable means for following the progress of the spheroidization reaction.

Before attempting metallographic examination of the cold worked Sn-Pb

material below room temperature by means of light optical methods or using a scanning electron microscope it was decided to use differential thermal analysis (DTA) to determine the temperature range in which the lamellar breakdown occurs. DTA experiments were attempted on specimens of 60Sn-40Pb cold rolled at -78°C (dry ice sublimation temperature). This has proved to be a most difficult task and, as yet, unsuccessful. The DTA technique depends upon detection of the small amounts of heat given off by an exothermic reaction (or heat absorbed by an endothermic reaction). Results to date on the Sn-Pb eutectic have been unreproducible and unmeaningful. The main sources of error being the very small amount of energy released during the spheroidization reaction and experimental noise occasioned by the condensation of traces of ice and its subsequent melting on the DTA specimens.

Some information has been gained from mechanical tests performed at -78°C . Eutectic Sn-Pb specimens were tested in compression using an Instron mechanical test machine. It has been found that as-cast lamellar specimens work soften during compression deformation, apparently this is a consequence of concurrent spheroidization. Test specimens initially with a spheroidized microstructure exhibit normal work hardening rather than work softening. Remarkably, this work softening behavior persists to -78°C , the lowest test temperature. This suggests that attempts to follow the isothermal progress of the spheroidization process would have to be carried out below -78°C (dry ice temperature). However, temperatures below -78°C in addition to being experimentally very difficult (for metallography, DTA, etc.) create another problem, the transformation of white, metallic Sn (BCT) to gray, non-metallic Sn (diamond cubic). This phase transformation is usually quite sluggish, and the white Sn phase (one of the two phases of the 60Sn-40Pb eutectic) can be undercooled far below the equilibrium temperature (13°C for pure Sn). At

-78°C there was no indication that deformation had stimulated the white to gray Sn transformation. But specimens cooled to -196°C were very brittle and broke up during attempts to roll them, probably because of the Sn transformation.

The experimental difficulties encountered plus the unexpected occurrence of the spheroidization reaction at temperatures as low as -78°C require some reassessment of the experimental aims. At this point it appears that further attempts to obtain quantitative kinetic data on the reaction of microstructural change from cold worked lamellar eutectic to spheroidized eutectic, should not be made. Clearly two experimental techniques have been successful, conventional optical metallographic characterization of the microstructures (at room temperature) and low temperature compression tests. These techniques will be used to demonstrate the influence of varying amounts of plastic strain applied over a range of temperatures on the resulting final spheroidized microstructure. Such information, while not so useful as quantitative isothermal kinetic data, will help to elucidate the process of lamellar breakdown both specifically in 60Sn-40Pb and generally in other lamellar microstructures.

IV. SYNTHESIS OF NEW TYPES
OF CATALYST MATERIALS

J. P. Collman

Professor of Chemistry

M. Boudart

Professor of Chemical Engineering
and Chemistry

and

W. A. Little

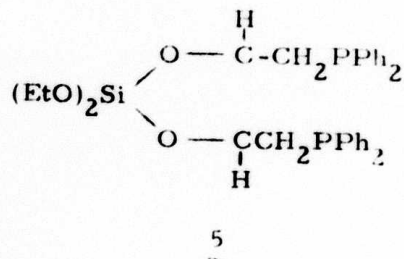
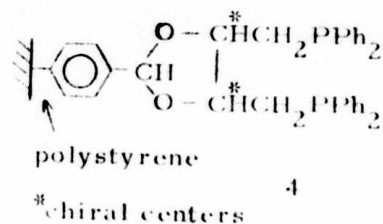
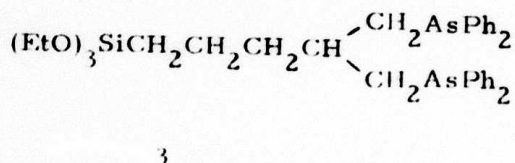
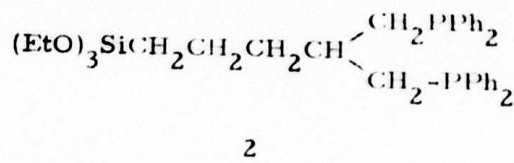
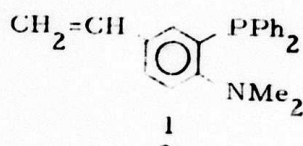
Professor of Physics

A. HETEROGENIZED HOMOGENEOUS CATALYSTS

J. P. Collman

1. Heterogenized-Homogenized Hydrogenation Catalysts

During the past six months an effort directed towards the synthesis of a new silylated chelate 1 has been in progress. This synthetic effort is not yet complete. An improved method for preparing Marquardt's silylated chelating phosphine 2 is being developed. However efforts to prepare the arsenic analogue 3 have not been successful. Kagan¹ has described a chelating chiral phosphine 4 chemically attached to polystyrene. Work in progress is directed towards a silylated analogue 5 of Kagan's chiral ligand. Additional rate data concerning the effect of poisons on a commercial rhodium catalyst are still being determined. These data are consistent with the hypothesis that adjacent surface rhodiums are necessary for each catalytic sequence.

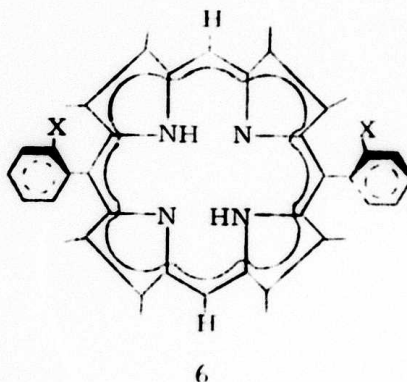


2. Metallic Catalyst Supports

Monodispersed solutions of 2H-TaS_2 have been prepared according to Murphy's directions^{2,3}. Rhodium(III) cations have been attached to the surface of these layered metals by ion exchange. Preliminary electrochemical studies⁴ of 2H-TaS_2 as single crystals and reprecipitated aggregates have been initiated. The two types of samples gave similar behavior but the potential range in which these materials remain "innocent" and will serve as inert electrode supports is limited to the cathodic side.

3. Face to Face Porphyrin Synthesis

Present efforts are directed towards the preparation of a key intermediate 6 which can be used to make a range of "face to face" porphyrins which we expect will catalyze multielectron redox reactions. At present we are three steps away from 6 in a six stage linear sequence.



4. References

- (1) H. B. Kagan and T. P. Dang, J. Am. Chem. Soc., 94, 6429 (1972).
- (2) D. W. Murphy and G. W. Hull, Jr., J. Chem. Phys., in submission (1974) and D. W. Murphy, F. J. DiSalvo, G. W. Hull, Jr., J. V. Waszczak, S. F. Meyer, G. R. Stewart, S. Early, J. V. Acrivos, and T. H. Geballe, J. Chem. Phys. in submission (1974).
- (3) We are indebted to Professor T. H. Geballe, Applied Physics Department for advice on the preparation of 2H-TaS_2 .
- (4) This work was carried out by M. Marrocco in Professor Fred Anson's laboratory at Caltech.

B. Supported Multimetallic Clusters

M. Boudart

1. Structure of Small Metallic Particles

Anisotropy is the most distinctive property of crystalline matter. Surface anisotropy of a large crystal is determined by its individual faces. In the case of catalytic particles in the nanometer range the notion of face is inadequate as revealed by electron microscopy. It is preferable to describe surface structure by specifying the fraction of surface atoms with a given number of nearest neighbors. A surface atom with i nearest neighbors is called C_i .

It has been shown theoretically by others that the surface structure of small particles changes with particle size in the range between 1 and 10 nm (1). For instance, the fraction of C_7 atoms at the surface of a bcc particle is almost ten times smaller on a 1 nm particle than on larger ones. Thus a study of the change in catalytic activity with particle size may establish whether a reaction depends on surface structure. If so, it is said to be structure sensitive. This appears to be the case for ammonia decomposition which proceeds at a rate 10 times higher on the (111) faces than on the (100) or (110) faces of tungsten single crystals (2). It must be noted that among the low index faces of bcc tungsten, only the (111) face exhibits C_7 sites.

In the case of ammonia synthesis, it has been observed by Brill and Kurzidim (3) that the catalytic activity of small particles of bcc iron was higher when the magnetite, Fe_3O_4 , used to prepare the catalyst was reduced by dihydrogen in the presence of dinitrogen, than when it was reduced by dihydrogen alone. It was also observed with field emission microscopy that dinitrogen reconstructs an iron tip by adsorbing preferentially on (111) planes and increasing their extent (4). Hence, it was surmised by Brill and Kurzidim, that the role of dinitrogen in the reduction of magnetite to form a more active catalytic surface was to favor the appearance of (111) faces which, in turn, were assumed to possess a higher catalytic activity than other

faces for the ammonia synthesis. In view of these observations suggesting a catalytic anisotropy of iron surfaces for the ammonia synthesis, it was decided to study the rate of that reaction of very small particles of iron and the variation of the rate with particle size and catalyst pretreatment in the presence or in the absence of dinitrogen.

It was hoped that Mössbauer spectra of these small iron particles would bring information on the desirable surface structures in ammonia synthesis.

2. Supported Iron Samples: Chemisorption

Small (1.5 nm), medium size (4 nm) and large (30 nm) iron particles were prepared on a magnesium oxide support. The average iron particle size was determined by the selective chemisorption of carbon monoxide, following the method of Brunauer and Emmett (5). In an attempt to verify the dinitrogen induced reconstruction of iron surfaces, the reduced iron particles were treated in flowing ammonia at 670 K and atmospheric pressure so as to form a bulk nitride of iron, as shown by Mössbauer spectra. Following the ammonia treatment, the iron nitride was decomposed at the same temperature in a flow of dihydrogen. The sequence of nitride formation and decomposition will be called ammonia treatment for short.

It was found that the amount of carbon monoxide chemisorbed on the small iron particles decreased by ca. 10% as a result of the ammonia treatment. If we accept the views of Brunauer and Emmett on the chemisorption of carbon monoxide on the low index faces of iron, the observed decrease in chemisorption can be explained if the ammonia treatment increases the relative proportion of C_7 sites.

3. Structure Sensitivity of Ammonia Synthesis on Iron

The turnover number N , i.e., the number of ammonia molecules made per second per iron site titrated by carbon monoxide, was found to increase by at least one order of magnitude with particle size. As Mössbauer spectra gave no indication of appreciable electronic

interaction between metal and support, the effect of particle size suggests that the ammonia synthesis is a structure sensitive reaction. The effect can be explained by assuming that C_7 sites, which are less probable on the smaller particles (1), are responsible for a higher value of N. This explanation is supported by the observed increase in N following the ammonia treatment which also appears to increase the population of C_7 sites as indicated above from chemisorption data and below from Mössbauer spectra.

4. Surface Magnetic Anisotropy of Small Ion Particles

In 1953, Néel predicted that sufficiently small particles should exhibit observable surface magnetic anisotropy as the latter becomes more important than shape and crystalline magnetic anisotropies which dominate with larger particles. This effect could be observed unequivocally for the first time in this work. Indeed, Mössbauer spectra of the smaller iron particles show that the surface magnetic anisotropy barrier is lowered by the ammonia treatment. From Néel's theory, it follows that the ammonia treatment increases the relative proportion of either C_5 or C_7 sites.

5. Conclusion

Three effects of surface anisotropy have been observed in this work: first, the decrease of CO chemisorption as a result of ammonia treatment, the increase of N with particle size and ammonia treatment and third, the decrease in surface magnetic anisotropy following ammonia treatment. All three taken together indicate that C_7 sites are formed as a result of ammonia treatment and are more active than the other sites in ammonia synthesis on iron. The ultimate explanation of this conclusion remains to be found. As of now, let us cite a remark of Selwood (7) who pioneered the study of magnetic and in particular superparamagnetic phenomena in chemisorption and catalysis: "It is remarkable that a development in geophysics plus one in the precipitation hardening of metals should have applications in heterogeneous catalysis." We submit that this remark provides some justification in talking about "the physical basis of catalysis."

6. References

- (1) R. van Hardeveld and F. Hartog, Surface Sci. 15, 189 (1969).
- (2) J. McAllister and R. S. Hansen, J. Chem. Phys. 59, 414 (1973).
- (3) R. Brill and J. Kurzidim, Colloques Int. CNRS 187, 99 (1969).
- (4) R. Brill, E. L. Richter, and E. Ruch, Angew. Chem. Intern. Ed. 6, 882 (1967).
- (5) S. Brunauer and P. H. Emmett, J. Am. Chem. Soc. 62, 1732 (1940).
- (6) L. Néel, J. Phys. Radium 15, 225 (1954).
- (7) P. W. Selwood, Adsorption and Collective Paramagnetism, Academic Press, New York 1962, p. 39.

C. Preparation of Fine Particles

W. A. Little and J. W. Brill

The objective of this research has been to prepare fine particles (20-1000⁰A) of controlled size distribution of various metals and to coat these with different organic or inorganic materials. These materials are expected to have novel electric, magnetic and mechanical properties which we plan to measure.

Progress to date

Particles have been prepared of Al, Au, Ni, Cu and Fe by evaporating the metal in an atmosphere of Argon or Helium. An extensive electron microscope study was made of the size distribution of the particles by collecting them on electron microscope grids and covering them with a carbon film. Some samples were found to have an amorphous coating but "clean" samples could be formed by placing a shutter between filament and grid and only opening the shutter for a fraction of a second.

Experiments have been done to see if efficient collection of Iron particles can be made using a suitably shaped magnetic field. Thick webs of particles could be formed but collection efficiency was generally found not to be good. Alternative ways of producing fine coated particles by grinding under suitable chemicals have been considered.

The possibility of studying the plasmon states of individual fine metal particles is being considered and preliminary experiments

have been done using the essential elements of a characteristic energy loss spectrometer. It is anticipated that such studies might clarify the role of particle size on chemical reactivity.

V. DEVELOPMENT OF ELEVATED TEMPERATURES
ELECTROCRYSTALLIZATION TECHNIQUES

R. S. Feigelson

Director, Crystal Technology
Center for Materials Research

and

R. A. Huggins

Professor of Materials Science
and Engineering

A. Introduction

The majority of work reported in the literature on electrochemical crystallization has been concerned with the synthesis of various compounds, primarily of the transition elements and the preparation of metallic coatings for commercial applications. Very little effort, however, has been expended on the development of a sufficiently sophisticated understanding of the principles involved in the technique to allow adequate control of the nucleation and growth processes necessary for the production of useful bulk samples including single crystals of a wide range of materials. In order to achieve this level of control, it is necessary to understand how to produce and maintain the appropriate thermodynamic and kinetic conditions at the growth interface during the electrocrystallization process. It is in this direction that the major emphasis of this program is oriented. One of the outgrowths of this effort will be the ability to produce material continuously including single crystals by refined electrochemical crystallization techniques.

Attention is also being given to the development of the electrochemical conditions necessary for the production of a group of specific materials of special interest. These include intermetallic niobium compounds with high superconducting transition temperatures, high melting point boride compounds with unusual hardness and good electron emissivities, and other materials of interest because of their potential technological use as optical materials or mixed conductors in new types of battery systems.

During this report period, significant achievements have been made. Large single crystals of Na_xWO_3 have been produced by the electrochemical crystallization method under controlled conditions using molten tungstate baths and a Czochralski-like growth technique. The superconducting phase Nb_3Ge has been synthesized by electrolysis of a molten salt bath.

A system capable of reproducibly growing LaB_6 single crystals from molten salt baths has been developed.

Each of these programs will be discussed separately in the following sections.

B. Investigation of the LaB_6 System

I. V. Zubeck and P. A. Pettit

1. Introduction

Very little previous effort has gone into the development of a sufficiently sophisticated understanding of the principles involved in electrocrystallization to allow the production of useful bulk samples, and single crystals. The emphasis of this part of the program has been to understand how to produce and maintain the pertinent thermodynamic and electrochemical conditions necessary for morphology control.

The borides were chosen as a prototype system for metal-metalloid formation. The growth of lanthanum hexaboride (LaB_6) single crystals, selected because of its commercial interest, is presently being studied with emphasis on obtaining controlled growth conditions.

During the first phase of this program, techniques were developed which allowed the growth of small crystals of LaB_6 from a molten oxyfluoride bath on gold electrodes. From these early experiments the effect of process parameters on morphological stability, nucleation rate, deposition efficiency were extensively studied. The need for more sophisticated processing equipment along with a knowledge and control of reaction chemistry was recognized as an important requirement for the attainment of reproducible results. Efforts toward this goal have been realized during the past six months.

2. Experimental Results

Larger crystals of LaB_6 , 4 mm on a side, have been produced during this reporting period. This is a substantial improvement over previously reported results. The improvement in crystal size was made possible by modified experimental equipment capable of providing accurate control of growth parameters. A new furnace has provided a flatter temperature gradient in the region of the crucible. Installation of a temperature controller has allowed regulation of furnace temperature to within $\pm 0.5^\circ\text{C}$. A new P.A.R. research model potentiostat

galvanostat has provided a very stable accurate potential source. Cell potential can now be controlled over a wide current range, and a capability is provided for control and monitoring of a third electrode. Voltage measurements (overpotential) made between a floating third reference electrode and cathode, yielded valuable kinetic and thermodynamic information concerning the cathode process. With the third electrode used as a controlling electrode, a preset voltage (overpotential) between the reference electrode and cathode insures stability of the cathode process, a condition which is important for the growth of single crystals of high quality.

Sources of bath contamination within the system, which included the Furnace, Flange, Fittings, and crucible, have been identified, and are being systematically eliminated. Nickel crucibles have been replaced by glassy carbon and platinum.

A nucleation study has shown that when controlled growth conditions are achieved, grain selection does occur after crystallites have nucleated on the electrode (see Fig. 1). Under these more stable conditions, secondary nucleation does not interfere with the growth process. This is favorable to the growth of larger single crystals of improved quality and morphology.

The interrelationships among cell potential, cell current, and electrode configuration are now well understood and growth conditions are now reproducible. Cell potential is held constant during any given run, and cell current and resistance follow Ohm's law:

$$E = IR \quad \text{where } R = \frac{\rho l}{A}$$

$$E = I \frac{\rho l}{A}$$

ρ = resistivity
 l = distance between electrodes
 A = f (cathode area, anode area)

If we assume that the resistivity ρ of a solution remains constant during a run (bath not run to depletion) then we can write

$$E = \text{constant}$$

$$\frac{E}{\rho l} = \frac{I}{A} = \text{constant}$$



Figure 1. LaB_6 grown on Au substrate: 100X
Light area Au electrode, light grey LaB_6
crystallites, and the two phase dark grey
region the plastic sample mount.

if it is assumed that Δl is small compared with l . Thus, operation of an electrolysis cell at constant potential E implies operation at constant cathodic current density i/A . The cell current rises during a run as deposited material increases the effective cathode area (A increases), anode area being constant. This argument also implies that for constant cell potential E and a given initial cathode area, the cathode current density used during a run can be chosen by suitable choice of anode area. If $A_1 > A_2$, then $i_1 > i_2$ by $E = i = \text{constant}$.

The two growths shown on the graph in Fig. 2 were identical except for a difference in anode area. i_0 represents the initial current as measured ten minutes after the start of electrolysis. The current rises rapidly during the first few hours of a run as crystallites nucleated on the smooth substrate result in a large percentage change in cathode area. The current rises more slowly during the remainder of a run as crystallites already nucleated continue to grow. The difference in i_0 , rise time, final current and number of coulombs passed as seen in Fig. 2, are attributable to the different anode area used in the two experiments.

The growth mechanism operating in the electrodeposition of materials like LaB_6 is now understood.⁽¹⁻⁷⁾ Layers approximately 1μ thick form at pyramidal "active centers" on the crystal face and grow outward in all directions (Fig. 3a, b, c). At low to moderate current densities, these centers are located at the interior of the crystal faces. As the current density is increased the active centers shift to the corners and edges of the crystal (Fig. 4). At high current densities, corner growth results in distorted cubes and finally dendritic growths along the $[111]$ direction (Fig. 5a, b). The critical current density for the growth of crystals of cube shape appears to be in the region of 30 mA/cm^2 . The optimum current density for growth of single crystals appears to lie in the region from 10 to 25 mA/cm^2 . In addition, the effects of bath purity on the growth mechanism are now better understood.

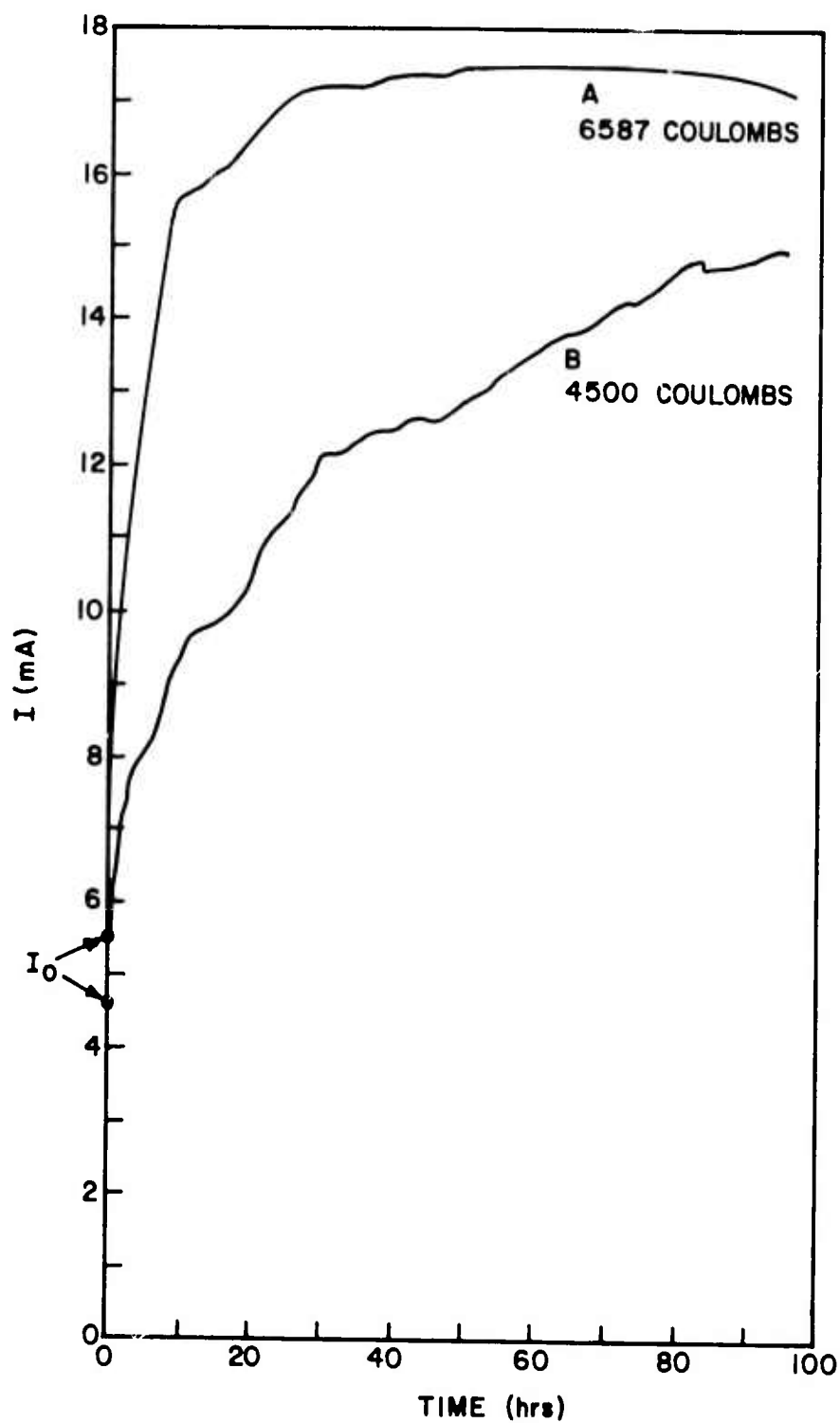


Figure 2. Current vs. time for LaB_6 growth using different anodes of different areas.



Figure 3a. Small crystallites, $\sim 10\mu$ on a side, showing exaggerated pyramidal structure at the face centers, 2000X.

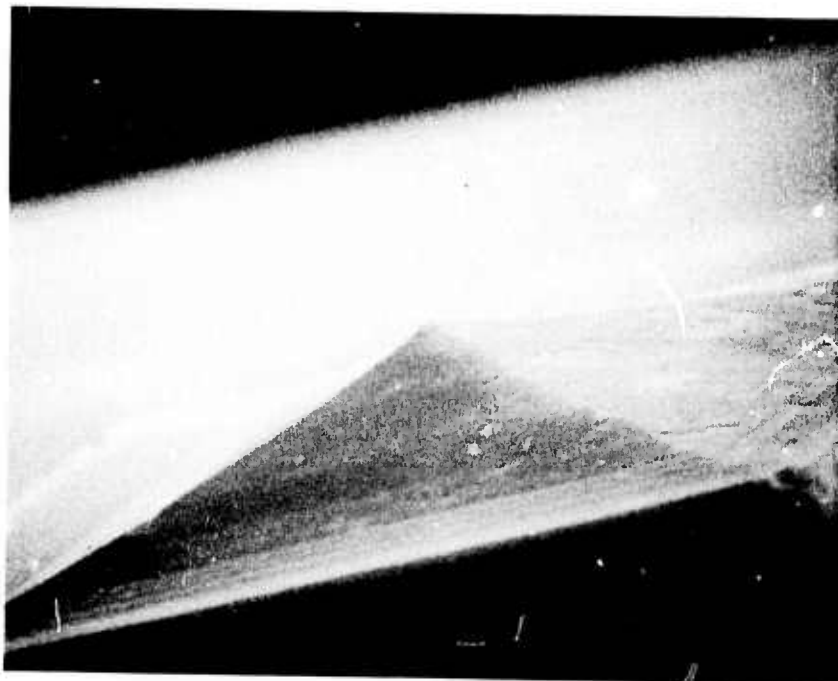


Figure 3b. Pyramidal growth structure, 5000X.

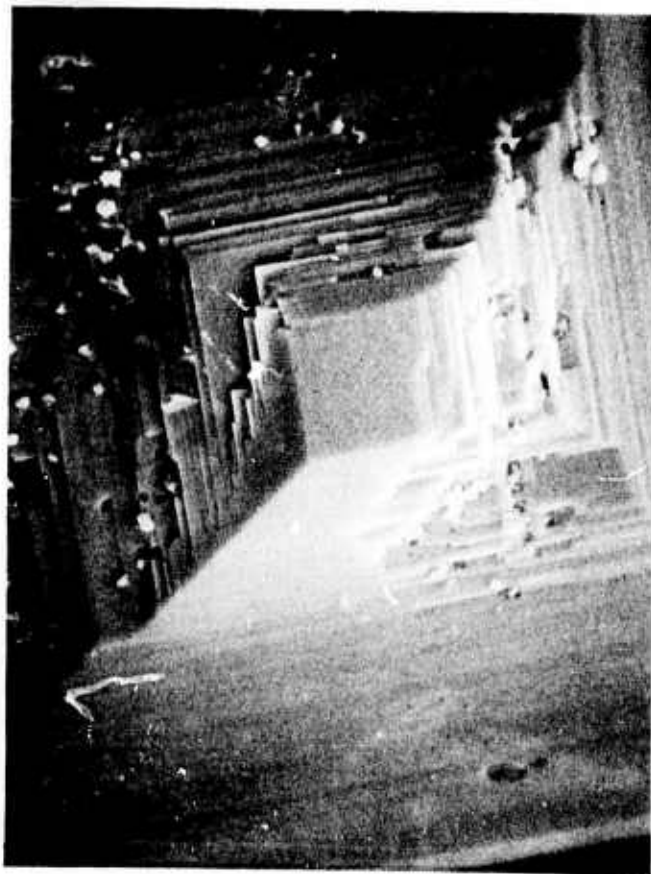


Figure 3c. Truncated pyramid with layers, 1000X.



Figure 4. Growth center at cube corner, $\sim 250\times$.



Figure 5a. Dendrites along $[111]$ direction,
composed of stacked cubes, evidence of
corner growth, 180X.



Figure 5b. Dendrites along $[111]$ direction, 500X.

3. Future Work

The LaB_6 program has proven fruitful in terms of demonstrating the influence of cell parameters on the growth process. Future work on this material will include seeded growth, growth at constant overpotential using the controlling reference electrode, and a study of the effect of melt purity on crystal size and quality. The influence of growth temperature and bath composition on defect structure, morphology and deposition efficiency will also be investigated. Electrochemical synthesis techniques developed in the course of the LaB_6 program are applicable to the preparation of other materials. An investigation of the synthesis of the scandium borides is planned for the next phase of the program.

4. References

- (1) A. Damjanovic, M. Paunovic, and J. O'M. Bockris, *J. Electro-analytical Chem.* 9, 93 (1965).
- (2) G. Wranglin, *Electrochem. Acta.* 2, 130 (1960).
- (3) H. J. Pick, G. G. Storey, and T. B. Vaughn, *Electrochim. Acta.* 2, 165 (1960).
- (4) T. B. Vaughn and H. J. Pick, *Electrochim. Acta.* 2, 179 (1960).
- (5) H. Fischer, *Electrochim. Acta.* 2, 50 (1960).
- (6) H. Seiter, H. Fischer, and L. Albert, *Electrochim. Acta.* 2, 97 (1960).
- (7) D. Elwell, I. Zubeck, R. Felgelson, and R. Huggins, to be published.

C. Continuous Growth

R. DeMattei

1. Introduction

The first year's activities were concerned with the factors which influence the stability of the growth interface during electrochemical crystallization. A study of the electrolytic growth of copper from a potassium chloride (KCl) (46 m/o) - zinc chloride (ZnCl_2) eutectic melt containing 5 m/o cupric chloride indicated that stirring had a beneficial effect on deposit morphology and distribution. The data was not sufficient to develop a quantitative relationship. A second study concerned the electrodeposition of zinc in an ultrasonic field from an aqueous zincate (ZnO_2^{-2}) solution (10 w/o potassium hydroxide (KOH) in water with 0.1 mole per liter zinc oxide, and showed that ultrasonic energy caused a decrease in the cathodic overpotential which in theory could be attributed to a decrease in boundary layer thickness and/or to an increase in the effective diffusion coefficient. Both of the above systems proved to be of limited utility in a continuous growth program because the growth habit during electrodeposition was not well-defined.

To facilitate the goal of being able to continuously grow a composition by the electrochemical deposition process, a new system based on sodium tungstate (Na_2WO_4) - tungstic oxide (WO_3) melts was investigated. Large sodium tungsten bronze single crystals (Na_xWO_3 , $0.1 > x > 1$) with well-defined morphologies can be produced from these melts at relatively high growth rates in the presence of suitable electric potentials. The growth of such Na_xWO_3 crystals provides a better system for the investigation of the limits of interface stability than the copper or zinc systems, since it is much easier to alter the quality of crystals which can be readily grown under a wide range of conditions, than it is to improve the interface stability in a system which is far from yielding stable growth conditions.

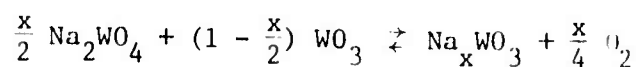
The major thrust of the program over the first half of this year has been toward the development of an understanding of and the techniques

for Czochralski-like growth of Na_xWO_3 via an electrochemical reaction in a tungstate melt under an applied electric potential.

2. Experimental Results

(a) Preliminary Experiments

Since the sodium tungsten bronze is formed by the reaction



it is known⁽¹⁾ that a growing crystal can be remelted if it comes in contact with free oxygen at high temperature. An apparatus designed to pull Na_xWO_3 from a melt, therefore, might require provisions for keeping the as-grown bronze crystal out of contact with oxygen. A series of experiments to test importance of the meltback problem and ways to prevent it were undertaken.

It was shown that a bronze crystal exposed to air at 750°C quickly melted back. In a flowing helium atmosphere the bronze was stable as long as oxygen bubbles generated at the anode did not come in contact with it. The oxygen formed at the anode did, however, float across the melt surface to the cathode where attack took place. To avoid this problem, the anode was enclosed in a compartment which doubled as a helium outlet.

(b) Apparatus

An apparatus for the combined Czochralski-electrochemical technique has been designed and constructed, Fig. 1. Pulling is accomplished using standard portable commercial crystal puller. In its present configuration, this unit is capable of pull rates from 1 to 6.5 mm/hr. Rotation of the seed is provided by a motor-generator driving through a speed reducer to provide rotation rates of 0 to 64 rpm. The crucible containing the melt is held in a quartz tube sealed by a water cooled brass flange. The flange is provided with fittings for both electrodes and introduction of an inert gas atmosphere, including a reference electrode for overpotential measurements, the

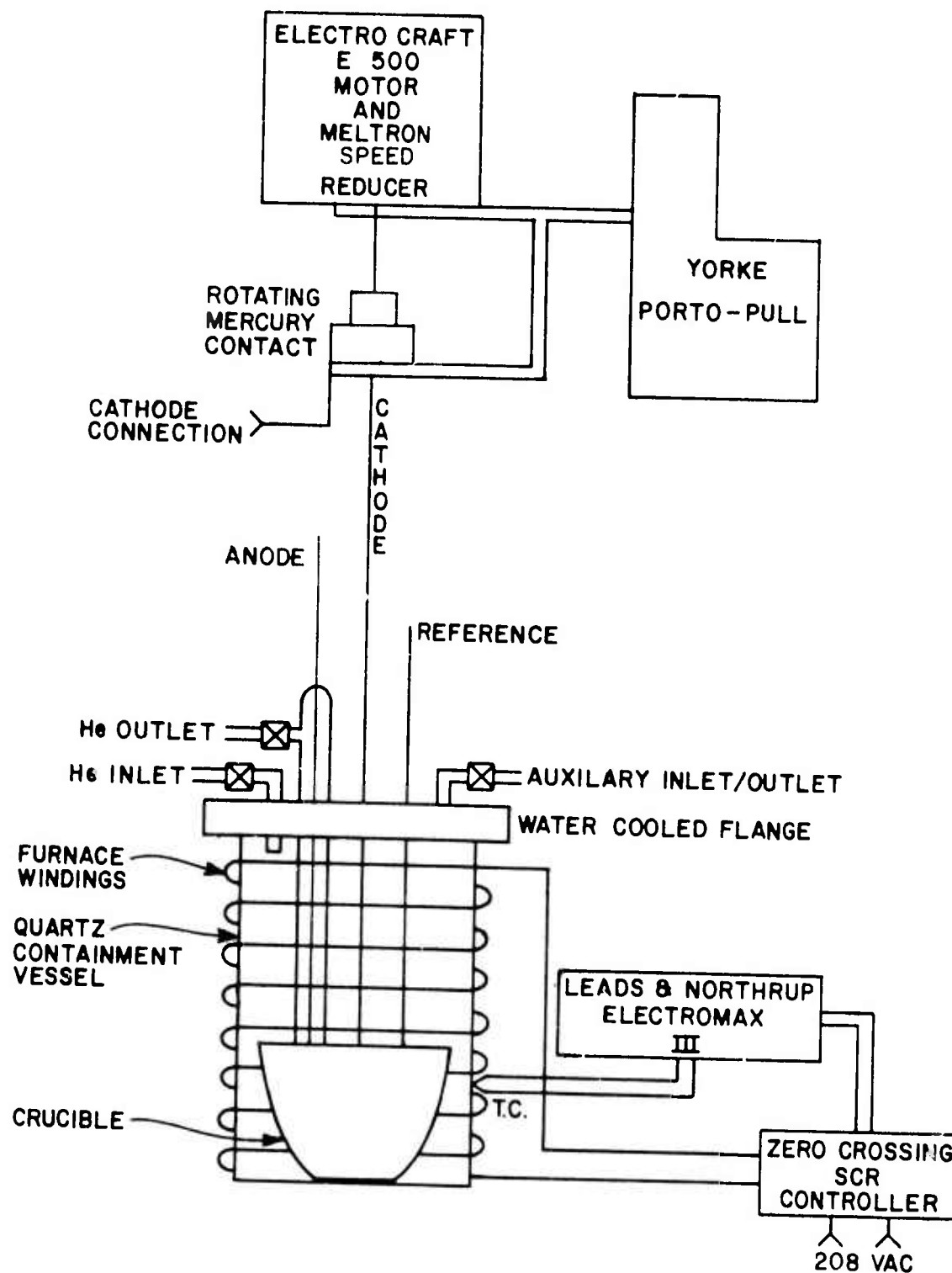


Figure 1. Diagram of the pulling-rotating mechanism and the furnace and controller of the Czochralski-electrochemical apparatus.

seed rod-cathode on which growth takes place, and the compartmented anode. The entire assembly fits inside a resistance furnace whose temperature is controlled by a three function proportional controller, which senses the wall temperature of the quartz tube by means of a chromel-alumel thermocouple. The average axial temperature gradient for this system is 13.5°C/cm.

The applied potential for electrodeposition is provided by a power supply which may be operated in either a constant voltage or a constant current mode. Contact to the rotating cathode is made through a mercury filled copper cup attached to the cathode rod. Measurements of both overpotential and applied cell potential are made with a voltmeter and the cell current is monitored by a clip-on milliammeter. All the electrochemical parameters are also recorded. See Fig. 2 for a block diagram of the circuit.

(c) Pulling Experiments

To date, several crystals of Na_xWO_3 have been pulled. All of these have been grown from a melt of 25 m/o WO_3 - 75 m/o Na_2WO_4 at 750°C under a flowing helium atmosphere. These growths were seeded with crystals grown in melts of the same composition indicated above. The longest crystal produced by this method is in excess of 7 cm in length. See Fig. 3.

When growing in a stable manner, these crystals exhibit a constant cross section. A model for this behavior may be derived by considering the volume of material deposited

$$v = \frac{\epsilon M a}{n F \rho}$$

where ϵ is the efficiency of the electrochemical process, M is the molecular weight of the species deposited, a is the total charge transferred, n is the number of electrons transferred (for Na_xWO_3 , $n = x$), F is Faraday's constant, and ρ is the density of the material. The rate of change of volume with time is given by

$$dv/dt = \frac{\epsilon M}{n F \rho} da/dt = \frac{\epsilon M}{n F \rho} I = KI$$

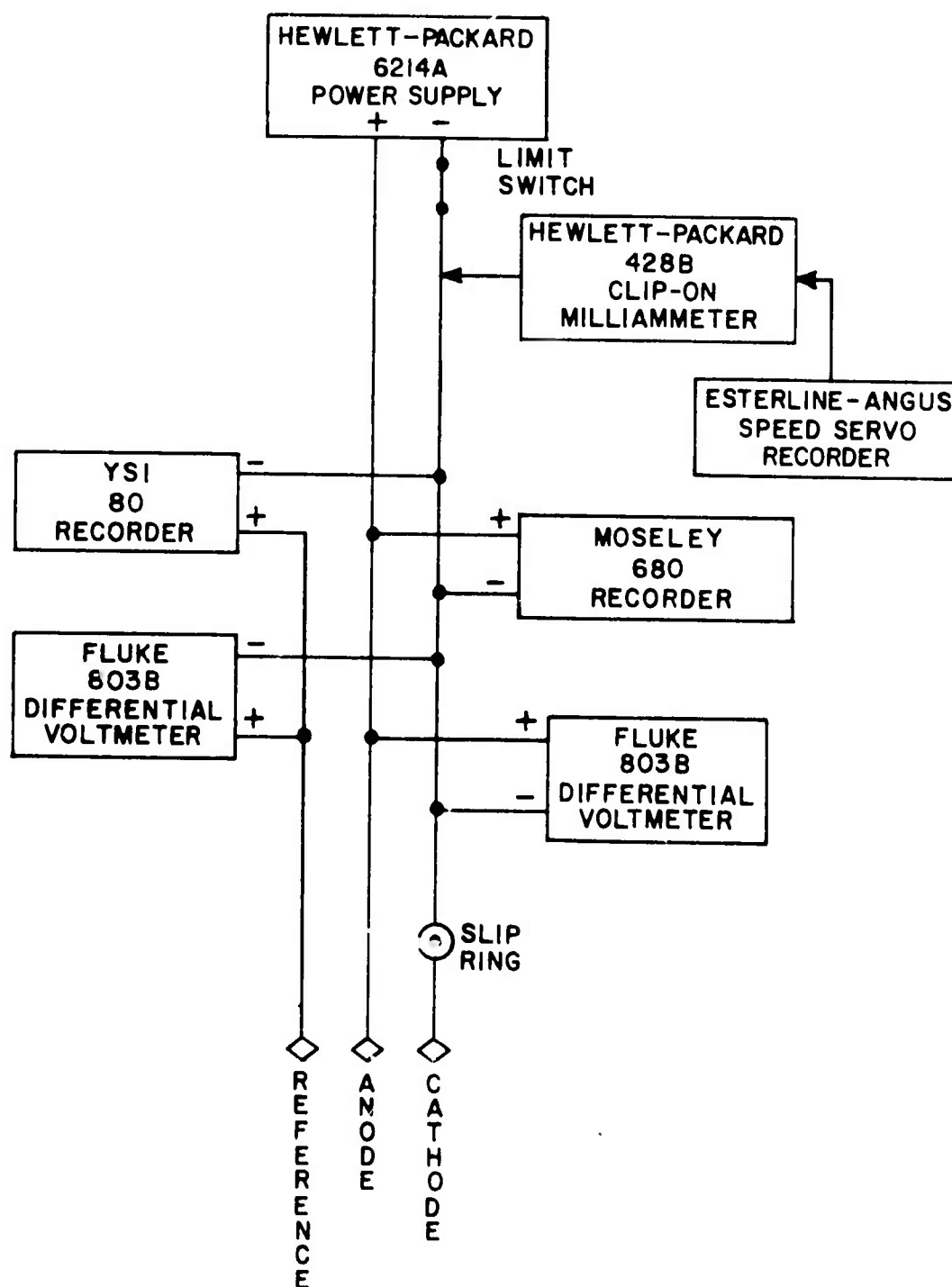


Figure 2. Block diagram of Electronics for Czochralski-electrochemical apparatus.

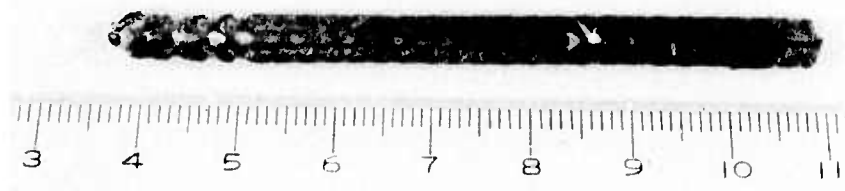


Figure 3. Section of $\text{Na}_{.8}\text{WO}_3$ crystal grown at 6.5 mm/hr at 64 rpm. Notches are due to periods of growth at reduced current.

where I is the total current. Volume may also be expressed as

$$v = Ay$$

where A is an area and y is a distance in the direction of pulling.

The rate of change of volume is

$$dv/dt = yda/dt + A dy/dt.$$

But at equilibrium, A is constant ($da/dt = 0$), thus

$$dv/dt = A dy/dt = KI.$$

In Na_xWO_3 in the cubic phase growing along the $[111]$, the interface is a trigonal pyramid the total area of which is

$$A = 3 d^2/4$$

where d is the distance across one of the crystal facets. Thus

$$d = \left(\frac{KI}{.75 \, dy/dt} \right)^{1/2}$$

where dy/dt is the pull rate. This model predicts that changing total current and pull rate in the same manner (i.e., doubling both) should leave the crystal cross section unchanged. In Fig. 4, a crystal is shown which demonstrates that constant cross section can be maintained by appropriate simultaneous changes in current and pull rate. The model further predicts that increasing the total current at a fixed pull rate will increase the cross section and increasing the pull rate at a fixed total current will decrease the cross section. An example of the former type of behavior is seen in Fig. 5, while the notches in Fig. 3 are an example of the latter type of behavior.

Crystals grown by the above procedure show a strong preference for growth along the $[111]$. Therefore, in most experiments, $[111]$ oriented seeds were utilized. In one growth using a seed oriented on the $[211]$, the boule axis grew off the seed axis and growth was found to be in the $[111]$ direction. Growth on other seed orientations have not yet been attempted.

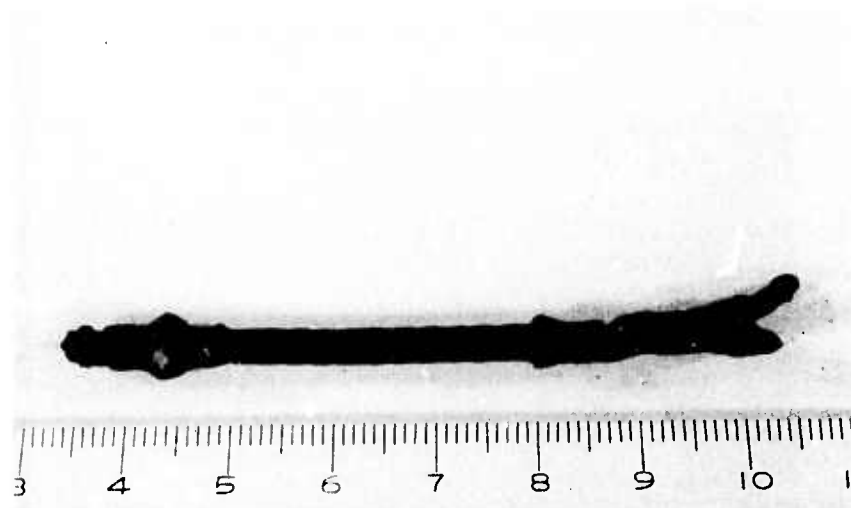


Figure 4. Example of $\text{Na}_{.8}\text{WO}_3$ crystal grown from 25 m/o $\text{WO}_3 - \text{Na}_2\text{WO}_4$ at 750°C . Starting at 4.4 cm:

- a) first 5.5 mm Current (I) = 7.5 ma,
 Pull rate (P) = 1 mm/hr.
- b) next 48.5 mm I = 15 ma, P = 1.95 mm/hr
- c) next 14.7 mm I = 22.5 ma, P = 2.95 mm/hr
- d) last 5 mm I = 37.5 ma, P = 5.1 mm/hr

Branching indicates that upper limit of stable growth has been reached. Rotation rate = 17.25 rpm.

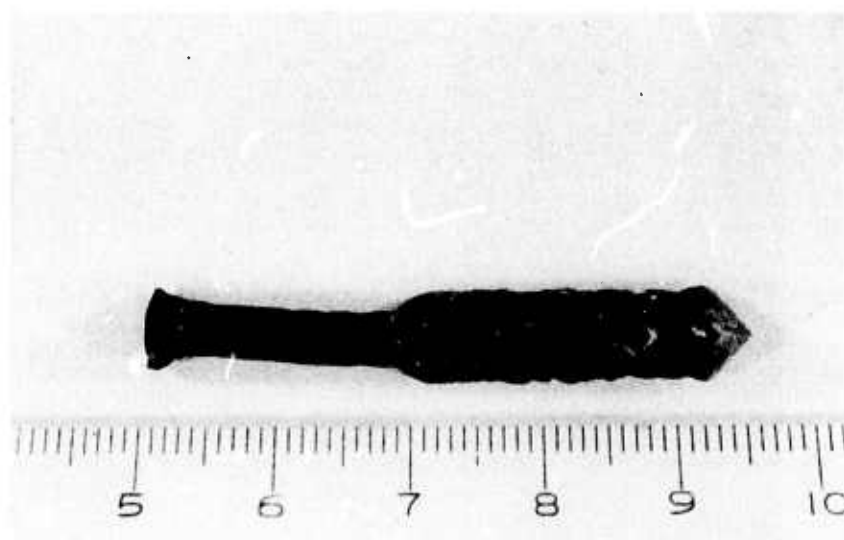


Figure 5. Example of a $\text{Na}_{.8}\text{WO}_3$ crystal grown at a constant pull rate (1 mm/hr) with a current increase. Rotation rate = 17.25 rpm.

a) Current (I) = 7.6 ma, Time (t) = 20 hrs

b) I = 15 ma, t = 23 hrs

(d) Rotation Experiments

As has been outlined in a previous report⁽²⁾ rotation of the growing crystal should produce beneficial effects. In the case of Czochralski-electrochemical growth, this should translate to higher pull rates. Preliminary experiments indicated that this was the case with the maximum allowable growth rate before onset of interface instability increasing from a maximum of 3.25 mm/hr at 16 rpm to in excess of 6.5 mm/hr at 64 rpm. For normal Czochralski growth of oxide materials a range of maximum stable pull rates from 2 mm/hr ($\text{Y}_2\text{Al}_5\text{O}_{12}$) to 10 mm/hr (ZnWO_4 , CaWO_4 , and LiTaO_3) has been observed.⁽³⁾

A further series of experiments to quantify the maximum pull rate versus rotation rate relationship is in progress. This series of experiments will also investigate the relationships between overpotential, current density and rotation rate.

3. Future Plans

In addition to the seed rotation experiments now in progress, the effects of stirring, applied ac potentials and ultrasonic energy on interface morphology and growth rate will be investigated along with studies on the influences of temperature, melt composition, and convective flow on growth parameters. Electrical measurement techniques will be developed to permit the accurate control of crystal size, quality, and growth rate. Other experiments planned include control of crystal shape, growth by controlling overpotential and continuous growth of materials of the LaB_6 type, which are representative of growth from solutions with low solute content.

A potentially important application of molten salt electrochemistry is in the area of epitaxial growth. The tungsten bronzes will allow the explorations of both homo- and heteroepitaxial techniques since the bronze lattice parameter changes with composition.

4. References

- (1) Private Communication - R. A. Huggins
- (2) R. DeMattei, Continuous Growth, Development of Elevated Temperature Electrochemical Crystallization Techniques, First Annual Report, Long Range Materials Research, Grant Number DAHC 15-73-G15, June 30, 1974, p. 158 ff.
- (3) J. C. Brice, Selected Topics in Solid State Physics, Volume XII, The Growth of Crystals From Liquids, North-Holland Publishing Co., London, 1973, p. 237.